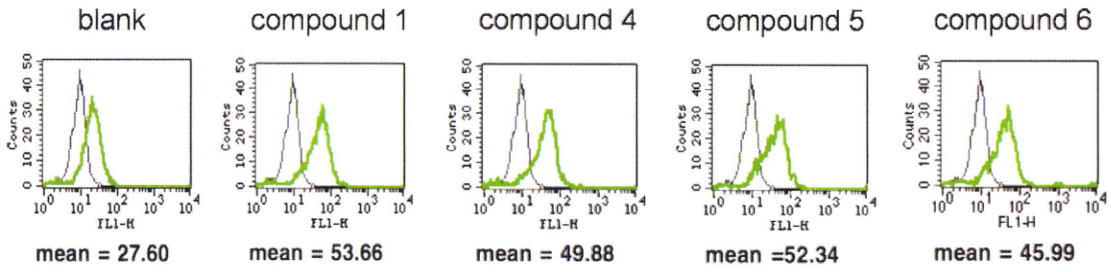

Figure 2. FACS analysis of compounds **1** and **4–6**. JR-FL (R5, Sub B) chronically infected PM1 cells were preincubated with 100 μM of a CD4 mimic for 15 min, and then incubated with an anti-HIV-1 mAb, 4C11, at 4 °C for 15 min. The cells were washed with PBS, and fluorescein isothiocyanate (FITC)-conjugated goat anti-human IgG antibody was used for antibody-staining. Flow cytometry data for the binding of 4C11 (green lines) to the Env-expressing cell surface in the presence of a CD4 mimic are shown among gated PM1 cells along with a control antibody (anti-human CD19:black lines). Data are representative of the results from a minimum of two independent experiments. The number at the bottom of each graph shows the mean fluorescence intensity (MFI) of the antibody 4C11.

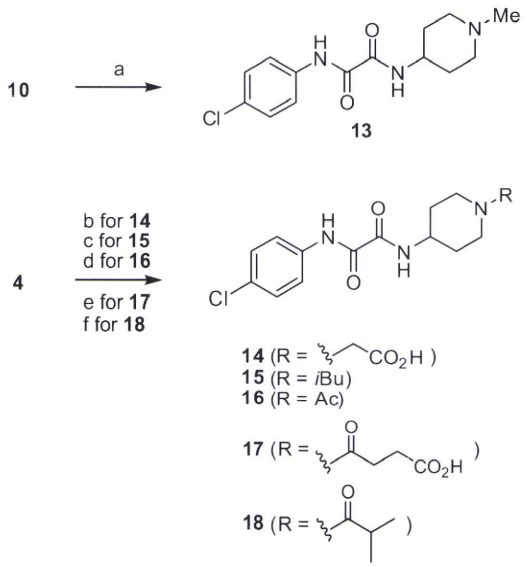

Scheme 2. Synthesis of N-alkylated and N-acylated piperidine derivatives **13–18**. Reagents and conditions: (a) 4-amine-1-methylpiperidine, EDC·HCl, HOBt·H_2O, Et_3N, THF, 16%; (b) (i) *tert*-butyl bromoacetate, NaH, DMF; (ii) TFA, 6%; (c) isobutylaldehyde, $NaBH(OAc)_3$, AcOH, DCE, quant.; (d) acetyl chloride, Et_3N, DMF, quant.; (e) succinic anhydride, Et_3N, THF, 37%; (f) isobutyric acid, EDC·HCl, HOBt·H_2O, Et_3N, THF, 95%.

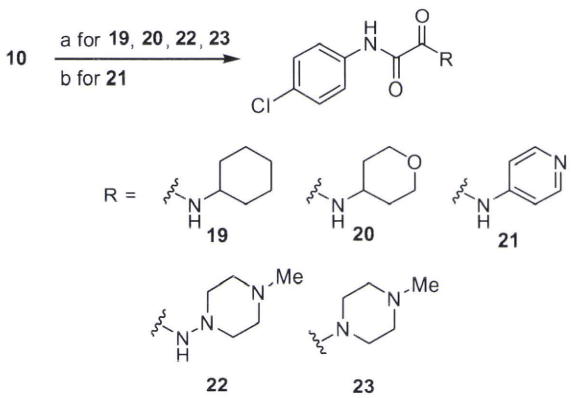

Scheme 3. Synthesis of 6-membered ring derivatives **19–23**. Reagents and conditions: (a) the corresponding amine, EDC·HCl, HOBt·H_2O, Et_3N, THF, 22%–quant.; (b) 4-aminopyridine, $SOCl_2$, MeOH, 38%.

ysis, and the results are shown in Figure 3. Pretreatment of the Env-expressing cells with the N-substituted compounds **13**, **15**, **16**, and **18** produced a notable increase in binding affinity to 4C11, similar to that observed in the pretreatment with compound **1**. The profile of the binding of 4C11 to the cell surface pretreated with compounds **14** and **17** was similar to that of controls, suggesting that these derivatives offer no significant enhancement of binding affinity for 4C11 and that the carboxylic moiety in the terminal of piperidine ring is not suited to CD4 mimicry. It is hypothesized that the carboxylic moieties of compounds **14** and **17** might prevent the interaction of CD4 mimic with gp120 by their multiple contacts with side chain(s) of amino acid(s) around the Phe43 cavity, such as Asp^{368} and Glu^{370}. Replacement of the piperidine moiety with the different 6-membered rings resulted in a significant loss of binding affinity for 4C11 in the FACS analysis of compound **19–23** (MFI(**19**) = 11.44, MFI(**20**) = 12.84, MFI(**21**) = 12.47, in MFI (blank) = 11.34; MFI(**22**) = 26.67, MFI(**23**) = 20.21, in MFI(blank) = 26.79, data not shown), indicating a significant contribution from the piperidine ring which interacts with gp120 inducing conformational changes.

In view of their ability to induce conformational changes of gp120, the anti-HIV activity and cytotoxicity of the piperidine derivatives **13–18** were further evaluated, with the results shown in Table 2. The anti-HIV activity of the synthetic compounds was evaluated against various viral strains including both laboratory and primary isolates and IC_{50} and CC_{50} values were determined as those of compounds **4–6**. The *N*-methylpiperidine compound **13**, was not found to possess significant anti-HIV activity against a primary isolate, but was found to possess moderate anti-HIV activity against a laboratory isolate, a IIIB strain (IC_{50} = 67 μM). Anti-HIV activity was not observed however, even at concentrations of 100 μM of **13** against an 89.6 strain. The potency was approximately eight-fold lower than that of the parent compound **1** (IC_{50} = 8 μM), indicating a partial contribution of the hydrogen atom of the amino group of the piperidine ring to the bioactivity of CD4 mimic. Although compound **15**, with an *N*-isobutylpiperidine moiety, failed to show significant anti-HIV activity against laboratory isolates, relativity potent activity was observed against a primary isolate, an MTA strain (IC_{50} = 28 μM). Compounds **16** and **18**, which are *N*-acylpiperidines, were tested against laboratory isolates and significant anti-HIV activity was not observed even at 100 μM. Compounds **14** and **17**, with the carboxylic moieties, failed to show significant anti-HIV activity against laboratory isolates even at 100 μM, which are compatible with the FACS analysis. These results suggest that the N-substituent on the piperidine ring of CD4 mimic analogs may contribute to a critical interaction required for binding to gp120. Compounds **19–23** showed no significant anti-HIV activity against a IIIB strain even at 100 μM, which are compatible with the FACS analysis (data not shown).

All but one of the compounds **13–18** have no significant cytotoxicity to PM1/CCR5 cells ($CC_{50} \geqslant 260$ μM); the exception is compound **18** (CC_{50} = 45 μM). Compounds **13** and **15** show relatively potent anti-HIV activity without significant cytotoxicity.

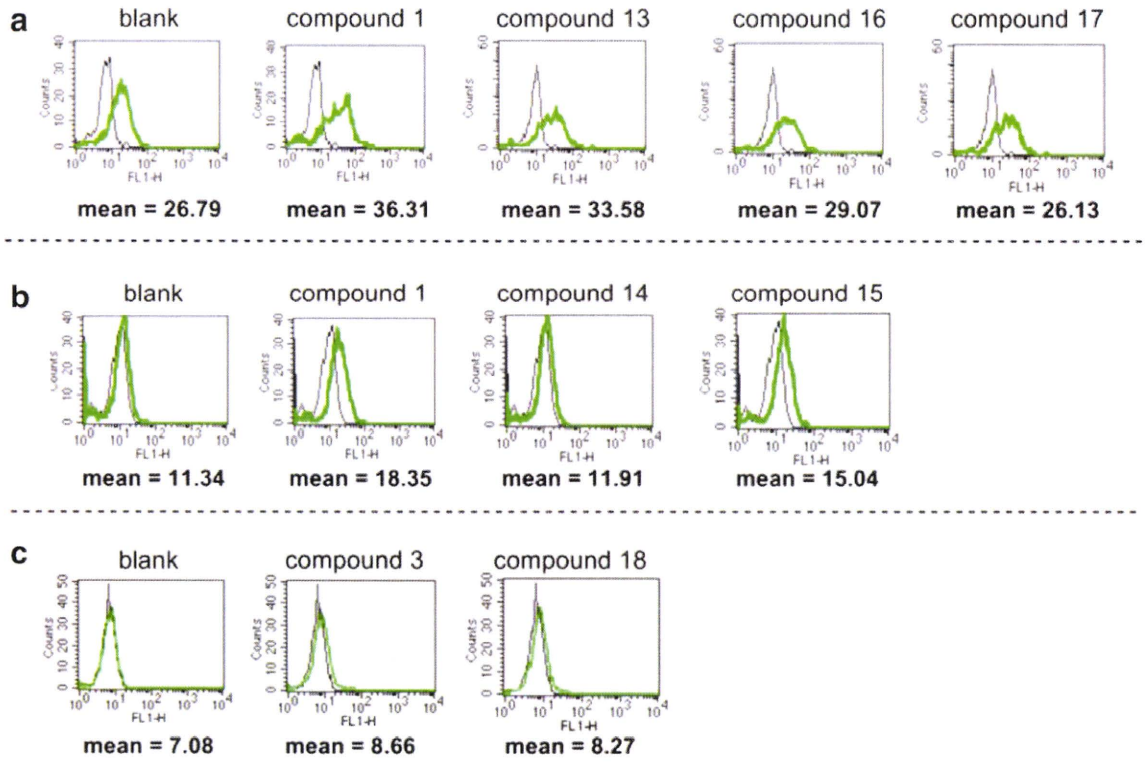

Figure 3. FACS analysis of compounds **1**, **3**, and **13–18**. The experimental procedures are described in Figure 2. The lanes of (a), (b) and (c) show independent experiments.

Table 2
Anti-HIV activity and cytotoxicity of compounds **13–18**[a]

Compd	R	IC_{50} (μM)			CC_{50} (μM)
		Laboratory isolates		Primary isolates	
		IIIB (X4)	89.6 (dual)	MTA (R5)	
1		8	10	ND	150
4	H	ND	ND	ND	100
13	Me	67	>100	ND	>300
14	CH_2CO_2H	>100	ND	ND	260
15	*i*Bu	>100	ND	28	>300
16	Ac	>100	>100	ND	>300
17	$C(O)CH_2CH_2CO_2H$	>100	>100	ND	>300
18	C(O)*i*Pr	>100	ND	ND	45

[a] All data with standard deviation are the mean values for at least three independent experiments.

The results for **15** showed it to have 3–6 times less cytotoxicity than **4** and **18**. This observation indicates that the alkylation of the piperidine nitrogen may be favorable because it lowers the cytotoxicity of CD4 mimic analogs.

In the course of the SAR studies on CD4 mimic analogs, we have already found that a CD4 mimic or sCD4 exhibited a remarkable synergistic effect[4e] with a 14-mer peptide CXCR4 antagonist T140.[9] This result indicates that the interaction of CD4 mimic with gp120 could facilitate the approach of CXCR4 to gp120 by exposing the co-receptor binding site of gp120. It was thought that the CD4 mimic analogs conjugated with a selective CXCR4 antagonist might as a consequence show a higher synergistic effect for the improvement of anti-HIV activity. In this context, efforts were made to synthesize and bioevaluate hybrid molecules that combined a CD4 mimic analog with 4F-benzoyl-TZ14011, which is a derivative of T140 optimized for CXCR4 binding and stability in vivo.[10]

The synthesis of hybrid molecules **27–29** is outlined in Scheme 4. To examine the influence of the linker length on anti-HIV activity and cytotoxicity, three hybrid molecules with linkers of different lengths were designed. Based on the fact that alkylation of the piperidine nitrogen, having no deleterious effects on bioactivity, is an acceptable modification of CD4 mimic analogs, the alkylamine moiety was incorporated into the nitrogen atom of the piperidine moiety to conjugate CD4 mimic analogs with 4F-benzoyl-TZ14011. Reductive alkylation of **4** with N^{α}-Boc-pyrrolidin-2-ol **24**, which exists in equilibrium with the corresponding aldehyde, and successive treatment with TFA and HCl/dioxane provided the amine hydrochloride **25**. Treatment of **25** with succinic anhydride under basic condition gave the corresponding acid **26**, which was subjected to condensation with the side chain of D-Lys[8] of 4F-benzoyl-TZ14011 in an EDC–HOBt system to give the desired hybrid molecule **27** with a tetramethylene linker.[11] Other hybrid molecules **28** and **29** bearing hexa- and octamethylene linkers, respectively, were prepared using the corresponding aldehydes **30** and **31**.

The assay results for these hybrid molecules **27–29** are shown in Table 3. To investigate the effect of conjugation of two molecules on binding activity against CXCR4, the inhibitory potency against

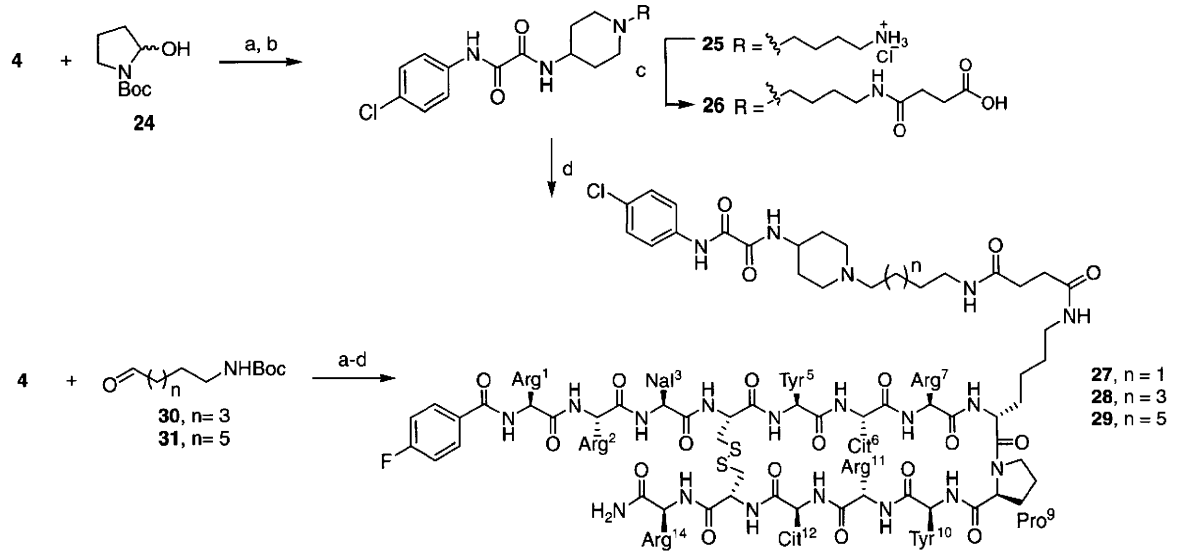

Scheme 4. Synthesis of hybrid molecules **27–29**. Reagents and conditions: (a) $NaBH(OAc)_3$, AcOH, DCE; (b) TFA, then 4 M HCl/1,4-dioxane; (c) succinic anhydride, pyridine, DMF, then 4 M HCl/1,4-dioxane; (d) 4F-benzoyl-TZ14011, EDC·HCl, $HOBt·H_2O$, Et_3N, DMF. Nal = L-3-(2-naphthyl)alanine, Cit = L-citrulline.

Table 3
CXCR4-binding activity, anti-HIV activity and cytotoxicity of hybrid molecules **27–29**[a]

Compd	EC_{50}[b] (μM)	IC_{50}[c] (μM)	CC_{50}[d] (μM)	SI (CC_{50}/IC_{50})
4F-benzoyl-TZ14011	0.0059	0.0131	ND	ND
1 (NBD-556)	ND	0 2.10	ND	19.2[e]
27 (C4)	0.0044	0.0509	8.60	169
28 (C6)	0.0187	0.0365	8.00	219
29 (C8)	0.0071	0.0353	8.60	244
AZT	ND	0.0493	ND	ND

[a] All data with standard deviation are the mean values for at least three independent experiments.
[b] EC_{50} values are based on the inhibition of [^{125}I]-SDF-1α binding to CXCR4 transfectants of CHO cells.
[c] IC_{50} values are based on the inhibition of HIV-1-induced cytopathogenicity in MT-2 cells.
[d] CC_{50} values are based on the reduction of the viability of mock-infected MT-2 cells.
[e] This value is based on the CC_{50} and IC_{50} values from Table 1.

binding of [^{125}I]-SDF-1α to CXCR4 was measured. All the hybrid molecules **27–29** significantly inhibited the SDF-1α binding to CXCR4. The corresponding EC_{50} values are: EC_{50}(**27**) = 0.0044 μM; EC_{50}(**28**) = 0.0187 μM; EC_{50}(**29**) = 0.0071 μM. These potencies are comparable to that of 4F-benzoyl-TZ14011 (EC_{50} = 0.0059 μM), indicating that introduction of the CD4 mimic analog into the D-Lys[8] residue of 4F-benzoyl-TZ14011 does not affect binding activity against CXCR4. Comparison of the binding activities of **27–29** showed that all hybrid molecules were essentially equipotent in inhibition of the binding of SDF-1α to CXCR4. This observation indicates that the linker length between two molecules has no effect on the binding inhibition.

Anti-HIV activity based on the inhibition of HIV-1 entry into the target cells was examined by the MTT assay using a IIIB(X4) strain. In this assay, the IC_{50} value of 4F-benzoyl-TZ14011 was 0.0131 μM. All hybrid molecules **27–29** showed significant anti-HIV activity [IC_{50}(**27**) = 0.0509 μM; IC_{50}(**28**) = 0.0365 μM; IC_{50}(**29**) = 0.0353 μM]; however, the potency was 2- to 4-fold lower than that of the parent compound 4F-benzoyl-TZ14011, indicating that the conjugation of CD4 mimic with a CXCR4 antagonist did not provide a significant synergistic effect. In view of the fact that the combinational uses of CD4 mimic with T140 produced a highly remarkable synergistic effect, the lower potency of hybrid molecules may be attributed to the inadequacy in the structure and/or the characters of the linkers. All the hybrid molecules **27–29** have relatively strong cytotoxicity [CC_{50}(**27**) = 8.6 μM; CC_{50}(**28**) = 8.0 μM; CC_{50}(**29**) = 8.6 μM]. However, selectivity indexes (SI = CC_{50}/IC_{50}) were 169 for **27**, 219 for **28**, and 244 for **29**, all 9–13 times higher than that of **1** (SI = 9.2). This result indicates that conjugation of a CD4 mimic analog with a selective CXCR4 antagonist can improve the SI of CD4 mimic.

The SAR study of a series of CD4 mimic analogs was conducted to investigate the contribution of the piperidine moiety of **1** to anti-HIV activity, cytotoxicity, and CD4 mimicry on conformational changes of gp120. The results indicate that (i) the methyl groups on the piperidine ring of **1** have no great influence on the activities of CD4 mimic; (ii) the presence of piperidine moiety is important for the CD4 mimicry; and (iii) N-substituents of the piperidine moiety contribute significantly to anti-HIV activity and cytotoxicity, as observed with N-alkyl groups such as methyl and isobutyl groups which show moderate anti-HIV activity and lower cytotoxicity.

Several hybrid molecules based on conjugation of a CD4 mimic with a selective CXCR4 antagonist were also synthesized and bioevaluated. All the hybrid molecules showed significant binding activity against CXCR4 comparable to the parent antagonist and exhibited potent anti-HIV activity. Although no significant synergistic effect was observed, conjugation of a CD4 mimic with a selective CXCR4 antagonist might lead to the development of novel type of CD4 mimic-based HIV-1 entry inhibitors, which possess higher selective indexes than a simple CD4 mimic. These results will be useful for the rational design and synthesis of a new type of HIV-1 entry inhibitors. Further structural modification studies of CD4 mimic are the subject of an ongoing project.

Acknowledgements

This work was supported by Grant-in-Aid for Scientific Research from the Ministry of Education, Culture, Sports, Science, and Technology of Japan, Japan Human Science Foundation, and Health and Labour Sciences Research Grants from Japanese Ministry of Health, Labor, and Welfare. T.T. and N.O. are grateful for the JSPS Reseach Fellowships for Young Scientist.

References and notes

1. Chan, D. C.; Kim, P. S. *Cell* **1998**, *93*, 681.
2. (a) Alkhatib, G.; Combadiere, C.; Broder, C. C.; Feng, Y.; Kennedy, P. E.; Murphy, P. M.; Berger, E. A. *Science* **1996**, *272*, 1955; (b) Choe, H.; Farzan, M.; Sun, Y.; Sullivan, N.; Rollins, B.; Ponath, P. D.; Wu, L.; Mackay, C. R.; LaRosa, G.; Newman, W.; Gerard, N.; Gerard, C.; Sodroski, J. *Cell* **1996**, *85*, 1135; (c) Deng, H. K.; Liu, R.; Ellmeier, W.; Choe, S.; Unutmaz, D.; Burkhart, M.; Marzio, P. D.; Marmon, S.; Sutton, R. E.; Hill, C. M.; Davis, C. B.; Peiper, S. C.; Schall, T. J.; Littman, D. R.; Landau, N. R. *Nature* **1996**, *381*, 661; (d) Doranz, B. J.; Rucker, J.; Yi, Y. J.; Smyth, R. J.; Samson, M.; Peiper, S. C.; Parmentier, M.; Collman, R. G.; Doms, R. W. *Cell* **1996**, *85*, 1149; (e) Dragic, T.; Litwin, V.; Allaway, G. P.; Martin, S. R.; Huang, Y.; Nagashima, K. A.; Cayanan, C.; Maddon, P. J.; Koup, R. A.; Moore, J. P.; Paxton, W. A. *Nature* **1996**, *381*, 667.
3. Feng, Y.; Broder, C. C.; Kennedy, P. E.; Berger, E. A. *Science* **1996**, *272*, 872.
4. (a) Zhao, Q.; Ma, L.; Jiang, S.; Lu, H.; Liu, S.; He, Y.; Strick, N.; Neamati, N.; Debnath, A. K. *Virology* **2005**, *339*, 213; (b) Schön, A.; Madani, N.; Klein, J. C.; Hubicki, A.; Ng, D.; Yang, X.; Smith, A. B., III; Sodroski, J.; Freire, E. *Biochemistry* **2006**, *45*, 10973; (c) Madani, N.; Schön, A.; Princiotto, A. M.; LaLonde, J. M.; Courter, J. R.; Soeta, T.; Ng, D.; Wang, L.; Brower, E. T.; Xiang, S.-H.; Do Kwon, Y.; Huang, C.-C.; Wyatt, R.; Kwong, P. D.; Freire, E.; Smith, A. B., III; Sodroski, J. *Structure* **2008**, *16*, 1689; (d) Haim, H.; Si, Z.; Madani, N.; Wang, L.; Courter, J. R.; Princiotto, A.; Kassa, A.; DeGrace, M.; McGee-Estrada, K.; Mefford, M.; Gabuzda, D., ; Smith, A. B., III; Sodroski, J. *ProS Pathogens* **2009**, *5*, 1; (e) Yamada, Y.; Ochiai, C.; Yoshimura, K.; Tanaka, T.; Ohashi, N.; Narumi, T.; Nomura, W.; Harada, S.; Matsushita, S.; Tamamura, H. *Bioorg. Med. Chem. Lett.* **2010**, *20*, 354; (f) Yoshimura, K.; Harada, S.; Shibata, J.; Hatada, M.; Yamada, Y.; Ochiai, C.; Tamamura, H.; Matsushita, S. *J. Virol.* **2010**, *84*, 7558.
5. Protein Data Bank (PDB) (entry 1RZJ).
6. Olofson, R. A.; Abbott, D. E. *J. Org. Chem.* **1984**, *49*, 2795.
7. The synthesis of compound **4**: To the solution of compound **10** (104 mg, 0.52 mmol) in dry THF (4.0 mL), Et_3N (159 μL, 1.15 mmol), $HOBt{\cdot}H_2O$ (87 mg, 0.57 mmol), EDCI·HCl (109 mg, 0.57 mmol) and 4-amino-1-benzylpiperidine (109 μL, 0.57 mmol) were added with stirring at 0 °C, and continuously stirred for 6 h with warming to room temperature under N_2 atmosphere. After concentration under reduced pressure, the residue was extracted with EtOAc. The extract was washed with aq saturated $NaHCO_3$ and brine, and dried over $MgSO_4$. Concentration under reduced pressure followed by flash chromatography over silica gel with $CHCl_3$–MeOH (20:1) including 1% Et_3N gave the crude benzyl amine as a white powder. To the solution of the above crude benzyl amine (95 mg, 0.26 mmol) in dry CH_2Cl_2 (10 mL), 1-chloroethyl chloroformate (110 μL, 0.68 mmol) was added dropwise with stirring at 0 °C. The mixture was then refluxed for 3 h under N_2 atmosphere. After concentration under reduced pressure, the residue was resolved in MeOH (10 mL) and then refluxed for 1 h. Concentration under reduced pressure gave a crude product. Reprecipitation with MeOH–Et_2O afforded a white powder of the title compound **4** (33 mg, 46% yield). δ_H(400 MHz; CD_3OD) 1.83–1.92 (2H, m, CH_2), 2.10–2.17 (2H, m, CH_2), 3.13 (2H, t, *J* 12.5, CH_2), 3.34 (1H, m, NH), 3.42–3.49 (1H, m, CH_2), 4.04 (1H, m, CH), 7.34 (2H, m, ArH), 7.51 (1H, m, NH), 7.73 (2H, m, ArH), 8.84 (1H, m, NH); LRMS (ESI), *m/z* calcd for $C_{13}H_{17}ClN_3O_2$ $(MH)^+$ 282.10, found 282.14.
8. Yoshimura, K.; Shibata, J.; Kimura, T.; Honda, A.; Maeda, Y.; Koito, A.; Murakami, T.; Mitsuya, H.; Matsushita, S. *AIDS* **2006**, *20*, 2065.
9. (a) Tamamura, H.; Xu, Y.; Hattori, T.; Zhang, X.; Arakaki, R.; Kanbara, K.; Omagari, A.; Otaka, A.; Ibuka, T.; Yamamoto, N.; Nakashima, H.; Fujii, N. *Biochem. Biophys. Res. Commun.* **1998**, *253*, 877; (b) Tamamura, H.; Hiramatsu, K.; Mizumoto, M.; Ueda, S.; Kusano, S.; Terakubo, S.; Akamatsu, M.; Yamamoto, N.; Trent, J. O.; Wang, Z.; Peiper, S. C.; Nakashima, H.; Otaka, A.; Fujii, N. *Org. Biomol. Chem.* **2003**, *1*, 3663.
10. Hanaoka, H.; Mukai, T.; Tamamura, H.; Mori, T.; Ishino, S.; Ogawa, K.; Iida, Y.; Doi, R.; Fujii, N.; Saji, H. *Nucl. Med. Biol.* **2006**, *33*, 489.
11. The synthesis of a hybrid molecule **27**: To the solution of compound **26** (2.6 mg, 4.6 μmol) in DMF (1.0 mL), Et_3N (26 μL, 92 μmol), $HOBt{\cdot}H_2O$ (3.5 mg, 23 μmol) and EDCI·HCl (4.5 mg, 23 μmol) were added with stirring at 0 °C, and stirred for 1 h at room temperature. To the mixture 4F-benzoyl-TZ14011 (15 mg, 4.1 μmol) was then added and the mixture was stirred for 24 h at room temperature under N_2 atmosphere. After concentration under reduced pressure, the residue was purified by reversed phase HPLC (t_R = 23 min, elution: a linear gradient of 27–31% acetonitrile containing 0.1% TFA over 30 min) to afford a fluffy white powder of the desired compound **27** (1.3 mg, 9.8%). LRMS (ESI), *m/z* 2621.20 $[M+H]^+$, calcd 2620.25.

Remodeling of Dynamic Structures of HIV-1 Envelope Proteins Leads to Synthetic Antigen Molecules Inducing Neutralizing Antibodies

Toru Nakahara,[†] Wataru Nomura,*[,†] Kenji Ohba,[‡] Aki Ohya,[†] Tomohiro Tanaka,[†] Chie Hashimoto,[†] Tetsuo Narumi,[†] Tsutomu Murakami,[‡] Naoki Yamamoto,[‡] and Hirokazu Tamamura*[,†]

Department of Medicinal Chemistry, Institute of Biomaterials and Bioengineering, Tokyo Medical and Dental University, 2-3-10 Kandasurugadai, Chiyoda-ku, Tokyo 101-0062, Japan, and AIDS Research Center, National Institute of Infectious Diseases, 1-23-1 Toyama, Shinjuku-ku, Tokyo 162-8640, Japan. Received November 16, 2009; Revised Manuscript Received February 28, 2010

A synthetic antigen targeting membrane-fusion mechanism of HIV-1 has a newly designed template with C3-symmetric linkers mimicking N36 trimeric form. The antiserum produced by immunization of the N36 trimeric form antigen showed structural preference in binding to N36 trimer and stronger inhibitory activity against HIV-1 infection than the N36 monomer. Our results suggest an effective strategy of HIV vaccine design based on a relationship to the native structure of proteins involved in HIV fusion mechanisms.

INTRODUCTION

Antibody-based therapy is one of the promising treatments for AIDS. In recent years, AIDS antibodies have been produced by immunization (*1*) and by de novo engineering of monoclonal antibodies (mAb) with molecular evolution tactics such as phage display (*2*). Despite enormous efforts, however, only a limited number of highly and broadly HIV-neutralizing human mAbs have been isolated and characterized. These antibodies include gp41 Abs, 2F5 (*3*–*6*) and 4E10 (*5*–*7*), and gp120 Abs, 2G12 (*8*) and b12 (*9*). gp41 is a transmembrane envelope glycoprotein, which is divided into an endodomain and an ectodomain by the transmembrane region; the latter contains a hydrophobic amino-terminal fusion peptide, followed by amino-terminal and carboxy-terminal leucine/isoleucine heptad repeat domains with helical structures (HR1 and HR2, respectively). In the membrane fusion process of HIV-1, these subunits form a "pre-bundle" complex. The HR1 and HR2 regions are termed the N-terminal helix (N36) and C-terminal helix (C34), respectively. These helices form a six-helical bundle consisting of a central parallel trimeric coiled-coil of N36 surrounded by C34 in an antiparallel hairpin fashion. In design of immunogens that elicit broadly neutralizing antibodies, a useful strategy is to produce molecules that mimic the natural trimer on the virion surface. Previous studies show that these molecules could be proteins expressed as a recombinant form or on the surface of particles such as pseudovirions or proteoliposomes (*10*–*12*). The X-ray crystallographic study of gp41 shows that the distances between any two residues at the N-terminus of N-region are almost equal at approximately 10 Å (Figure 1A). A chemically synthetic template could be useful in connection with the design of a peptidomimetic corresponding to the native structure of gp41. To date, several gp41 mimetics have been synthesized as inhibitors or antigens and subjected to inhibition or neutralization assays (*13*–*16*). However, the templates for assembly of these helical peptides contain branched peptide linkers, which are not exactly equivalent in length (*14*). The N-terminal peptides constrained by another threefold linker showed high affinity for C-terminal peptides, although its biological advantages have not been determined (*15*). The mimicry can be estimated using the broadly neutralizing mAbs; suitable mimetics will bind neutralizing mAbs efficiently, but they will bind non-neutralizing mAbs poorly. In the present study, we designed and synthesized a novel three-helical bundle mimetic, which corresponds to the trimeric form of N36. We investigated whether mice immunized with the equivalent trimeric form of N36 mimetic can produce antibodies with stronger binding affinity for N36 trimer than for N36 monomer. This approach demonstrates the possibility of producing structure-specific antibodies by immunization of synthetic antigens corresponding to the natural form of viral proteins.

EXPERIMENTAL PROCEDURES

Conjugation of N36REGC and the Template to Produce triN36e. Compound **6** (100 μg, 0.174 μmol) and N36REGC (3.4 mg, 0.574 μmol) were dissolved in a mixture of 300 μL of 200 mM acetate buffer (pH 5.2) and 300 μL of TFE under a nitrogen atmosphere, then TCEP·HCl was added. The reaction was stirred for 72 h at room temperature and monitored by HPLC. The ligation product (triN36e) was separated as an HPLC peak and was characterized by ESI-TOF-MS, *m/z* calcd for $C_{690}H_{1160}N_{226}O_{201}S_3$ 15933.1, found 15933.8. The purification was performed by reverse phase HPLC (YMC-Pack ODS-A column, 10 × 250 mm). Elution was carried out with a 40–50% linear gradient of acetonitrile (0.1% TFA) over 50 min. Purified triN36e, obtained in 16% yield, was identified by ESI-TOF-MS. The detailed synthesis of peptides is described in the Supporting Information (SI).

CD Spectra. CD measurements were performed with a J-720 circular dichroism spectrolarimeter equipped with a thermoregulator (JASCO). The wavelength dependence of molar ellipticity [*θ*] was monitored at 25 °C from 190 to 250 nm. Peptides were dissolved in 20 mM acetate buffer (pH 4.0) containing 40% MeOH (*23*, *24*). The experimental helicity was calculated as reported previously (*17*–*19*).

Immunization and Sample Collection. Six-week-old male BALB/c mice were purchased from Sankyo Laboratory Service Corp. (Tokyo, Japan) and maintained under specific pathogen-free conditions in an animal facility. The experimental protocol was approved by the ethical review committee of Tokyo Medical and Dental University. Freund incomplete adjuvant and PBS

* To whom correspondence should be addressed. E-mail: nomura.mr@tmd.ac.jp; tamamura.mr@tmd.ac.jp. phone: +81-3-5280-8036, fax: +81-3-5280-8039.

[†] Tokyo Medical and Dental University.

[‡] National Institute of Infectious Diseases.

10.1021/bc900502z
Published on Web 04/01/2010

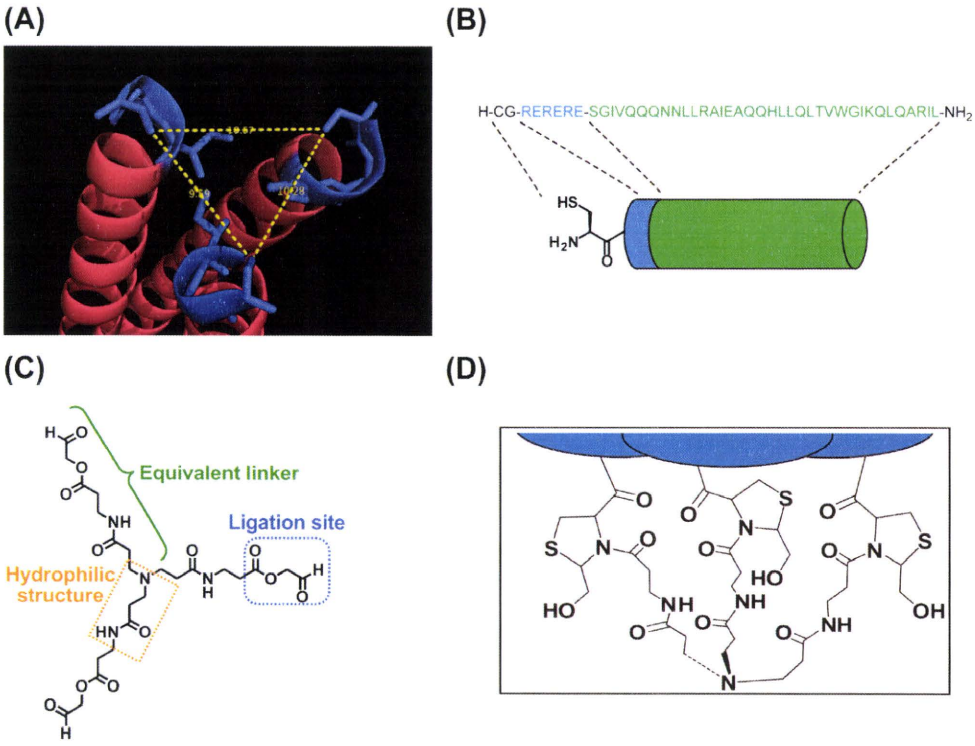

Figure 1. (A) Distances between hydrogen atoms for hydroxyl groups in N-terminal serine residues of N36 helices in trimeric form. The distances were evaluated by PyMOL (*21*). (B) Cartoon presentation of each N36 derived peptide, N36REGC. (C) Design of a C3-symmetric template. The amino acid residues are described in single letters. (D) Conjugated structure of trimeric N36 after thiazolidine ligation.

were purchased from Wako Pure Chemical Industries (Osaka, Japan). DMSO (endotoxin free) was purchased from Sigma-Aldrich (St. Louis, MO).

All mice were bled one week before immunization. One hundred micrograms of antigen was dissolved in 1 μL of DMSO. The solution was mixed with 50 μL of PBS and 50 μL of Freund incomplete adjuvant. The mixture was injected subcutaneously under anesthesia on days 0, 14, 28, 42, and 58. Mice were bled on days 21, 35, 49, and 65. Serum was separated by centrifugation (15 000 rpm) at 4 °C for 15 min and inactivated at 56 °C for 30 min. Sera were stored at −80 °C before use.

Serum Titer ELISA. Tween-20 (polyoxyethylene (20) sorbitan monolaurate) and hydrogen peroxide (30%) were purchased from Wako. ABTS (2,2-azino-bis(3-ethylbenzothiazoline-6-sulfonic acid) diammonium salt) was purchased from Sigma-Aldrich. Antimouse IgG (H+L)(goat)-HRP was purchased from EMD Chemicals (San Diego, CA). Ninty-six-well microplates were coated with 25 μL of a synthetic peptide at 10 μg/mL in PBS at 4 °C for overnight. The coated plates were washed 10 times with deionized water and blocked with 150 μL of blocking buffer (0.02% PBST, PBS with 0.02% Tween 20, containing 5% skim milk) at 37 °C for 1 h. The plates were washed with deionized water 10 times. Mice sera were diluted in 0.02% PBST with 1% skim milk, and 50 μL of 2-fold serial dilutions of sera from 1/200 to 1/102400 were added to the wells and allowed to incubate at 37 °C for 2 h. The plates were washed 10 times with deionized water. Twenty-five microliters of HRP-conjugated antimouse IgG, diluted 1:2000 in 0.02% PBST, was added to each well. After 45 min incubation, the plates were washed 10 times and 25 μL of HRP substrate, prepared by dissolving 10 mg ABTS to 200 μLof HRP staining buffer—a mixture of 0.5 M citrate buffer (pH 4.0, 1 mL), H_2O_2 (3 μL), and H_2O (8.8 mL)—was added. After 30 min incubation, the reaction was stopped by addition of 25 μL/well 0.5 M H_2SO_4, and optical densities were measured at 405 nm.

Virus Preparation. The pNL4-3 construct (8 μg) was transfected into 293T cells by Lipofectamine LTX (Invitrogen, Carlsbad, CA) followed by changing medium at 12 h after transfection. At 48 h after changing medium, the supernatant was collected, passed through a 0.45 μm filter, and stored at −80 °C as HIV-1_{NL4-3} strain before use. For titration, MT-4 cells were infected with serially 3-fold diluted virus from 1/10 to 1/196830, and cultured for 7 days. HIV-1 p24 levels in supernatants were measured, and then the titer of virus solution was calculated.

Anti-HIV Assay. Virus was prepared as described above except that the transfection of pNL4-3 was performed by the calcium phosphate method. Anti-HIV-1 activity was determined on the basis of protection against HIV-1-induced cytopathogenicity in MT-4 cells. Various concentrations of AZT, N36RE, and triN36e (The starting concentrations are 100, 10, and 1 μM, respectively) were added to HIV-1-infected MT-4 cells (MOI = 0.01) by 2-fold serial dilution and placed in wells of a flat-bottomed microtiter plate (2.0×10^4 cells/well). After 5 days' incubation at 37 °C in a CO_2 incubator, the number of viable cells was determined using the 3-(4,5-dimethylthiazol-2-yl)-2,5-diphenyltetrazolium bromide (MTT) method (EC_{50}). Cytotoxicity of compounds was determined on the basis of viability of mock-infected cells using the MTT method (CC_{50}). Each experiment was performed three times independently.

Neutralizing Assay. MT4-cells (1×10^5 cells/100 μL) were incubated in 100 μL medium containing 10 μL sera from immunized or preimmunized mice for 1 h at 37 °C, then pretreated MT-4 cells were infected with HIV-1_{NL4-3} (MOI = 0.05). At 3 days after infection, cells were collected by centrifuge at 4000 rpm for 10 min at 4 °C. After discarding supernatant, pellets were lysed with 30 μL of lysis buffer (50 mM Tris·HCl (pH 7.5), 150 mM NaCl, 1% NP-40), then 30 μL of 2 × SDS buffer (125 mM Tris·HCl (pH 6.8), 4% SDS, 20% glycerol, 10% 2-ME, 0.004% BPB) were added and boiled for 10 min. The samples (5 μL) were subjected to SDS-page to perform Western blotting. The HIV-1 gag p24 was detected by using Western lightning ECL kit (PerkinElmer, MA) according to manufacturer's instruction after treatment of HIV-1 p24

Scheme 1. Synthesis of the Equivalently Branched Template 6

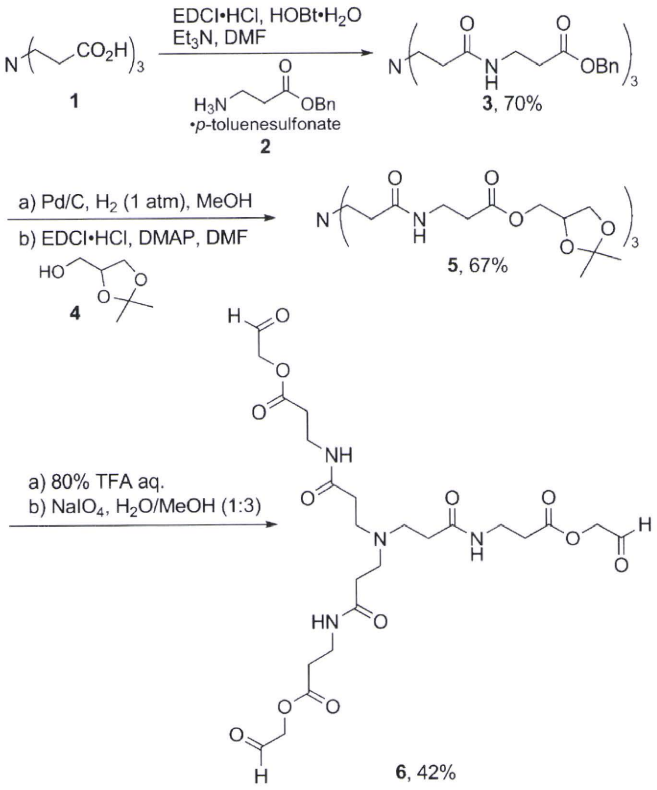

antibody (2C2; 1:2000 dilution) (*20*) and anti- mouse IgG (H+L)-HRP (Millipore, MA). The band intensity of p24 was calculated with post/pre-immunized samples by using *ImageJ* image analyzing software.

RESULTS AND DISCUSSION

The N-region of gp41 is known to be an aggregation site involving a trimeric coiled-coil conformation. In design of an N36-derived peptide (N36RE), the triplet repeat of arginine and glutamic acid was fused to the N-terminus to increase the solubility in buffer solution (Figure 1B). In order to form a triple helix corresponding precisely to the gp41 prefusion form, we designed the novel C3-symmetric template depicted in Figure 1C. This designed template linker has three branches of equal length and possesses the hydrophilic structure and ligation site for coupling with N36RE. The template was synthesized from the commercially available 3-[bis(2-carboxyethyl)amino]propanoic acid **1** as shown in Scheme 1. Coupling of **1** with β-alanine benzyl ester **2** gave the corresponding triamide **3** in 77% yield. Cleavage of three benzyl esters by hydrogenation and coupling with solketal **4** produced the corresponding triester **5**. Deprotection of the acetonides with aqueous 80% TFA followed by oxidative cleavage of diol group led to the desired template **6**. This approach uses thiazolidine ligation for chemoselective coupling of Cys-containing unprotected N36RE (N36REGC) with a three-armed aldehyde scaffold producing triN36e (Figure 1D). Thiazolidine ligation is a peptide segment coupling strategy which does not require side chain protecting groups (*22*−*26*). The reaction consists of three steps: (i) aldehyde introduction, in which a masked glycolaldehyde ester is linked to the carboxyl terminus of an unprotected peptide by reverse proteolysis; (ii) ring formation, in which the unmasked aldehyde reacts at acidic pH with the α-amino group of an N-terminal cysteine residue of the second unprotected peptide forming a thiazolidine ring; and (iii) rearrangement at higher pH in which O-acyl ester linkage is converted to an N-acyl amide linkage forming a peptide bond with a pseudoproline structure (Figure 2).

Circular dichroism (CD) spectra of triN36e and N36RE, which is a monomer form without N-terminal Cys-Gly residues, are shown in Figure 3A. The peptides were dissolved in 20 mM acetate buffer with 40% MeOH, pH4.0, suitable for measurement of CD spectra of membrane proteins (*27*, *28*). Both spectra display double minima at 208 and 222 nm and showed high molar ellipticity as absolute values (Table 1). The results indicate that these peptides form a highly structured α-helix and that the helical content of the trimer triN36e is higher than that of the monomer N36RE. Furthermore, to assess the interaction of triN36e with C34, CD spectra of the peptide mixture with C34-derived peptide, C34RE, were measured (Figure 3B,C). The spectrum of triN36e and C34RE mixture showed high molecular ellipticity as an absolute value comparable with that of triN36e alone. This supports the conclusion that C34RE interacts with tri36e and thereby induces a higher helical form as shown previously (*29*).

Mice were immunized with these synthetic gp41 mimetics and antibody production was successfully induced (the detailed titer increase in 5 weeks' immunization is given in the Supporting Information). Two out of three mice showed induction of antibodies against either antigen (N36RE or triN36e). Antibody titers and selectivity of antisera isolated from mice immunized with N36RE or triN36e were evaluated by serum titer ELISA against coated synthetic antigens. The most active antiserum for each antigen was utilized for the evaluation of binding activity by ELISA (Figure 4). The N36RE-induced antibody showed approximately 5 times higher affinity for N36RE than for triN36e, as 50% bound serum dilutions are 3.88×10^{-4} and 2.14×10^{-3} to N36RE and triN36e, respectively. It is noteworthy that the triN36e-induced antibody showed approximately 30 times higher preference in binding affinity for triN36e antigen than for N36RE (serum dilutions at 50% bound are 3.83×10^{-3} to N36RE and 1.33×10^{-4} to triN36e). Although this evaluation was not determined with purified mAbs, it is clear that the antibodies produced exploit a structural preference for antigens. The mechanism of induction

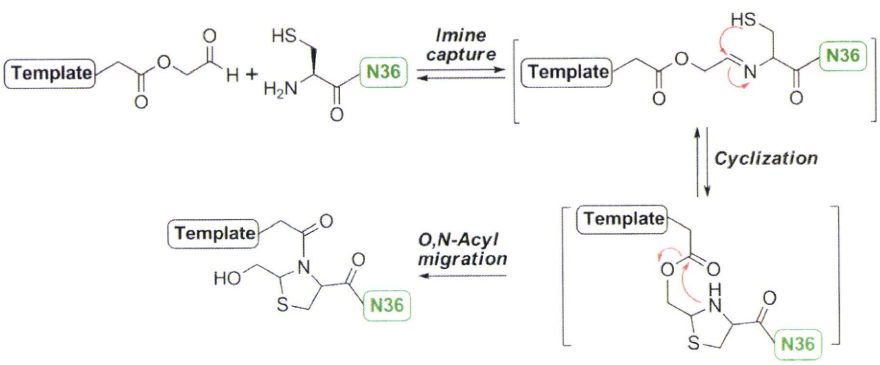

Figure 2. Reaction mechanisms of thiazolidine ligation utilized for assembly of N36RE helices on the template.

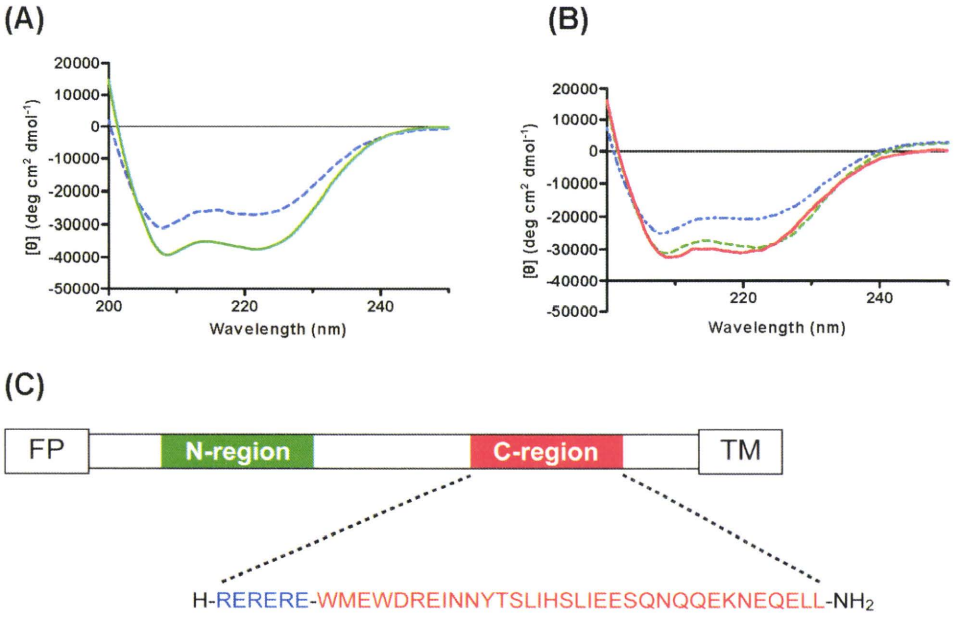

Figure 3. (A) Circular dichroism (CD) spectra of N36RE and triN36e. In the spectra, a blue dashed line and a green line show N36RE (monomer) and triN36e (trimer), respectively. Concentrations of the peptides are 10 and 3.3 μM for N36RE and triN36e, respectively. (B) CD spectra in the presence or absence of C34RE peptide. The spectra show the following: a dashed green line, triN36e; a dashed blue line, C34RE; a red line, triN36e+C34RE, respectively. The concentrations of peptides were as follows: triN36e (2.3 μM), C34-derived peptide C34RE (7 μM), and mixture of both peptides (3.5 μM each). (C) The amino acid sequence of C34RE described in single letters. FP and TM represent hydrophobic fusion peptide and transmembrane domain, respectively.

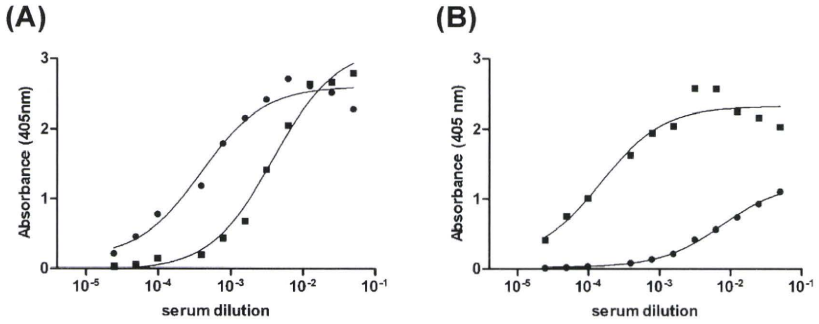

Figure 4. Serum titers of antibodies produced by N36 monomer and conformationally constrained N36 trimeric antigen. The titers were evaluated against N36RE (monomer) (A) and triN36e (trimer) (B). The plots indicate the results of sera obtained from N36RE-immunized mouse (•) and triN36e-immunized mouse (■).

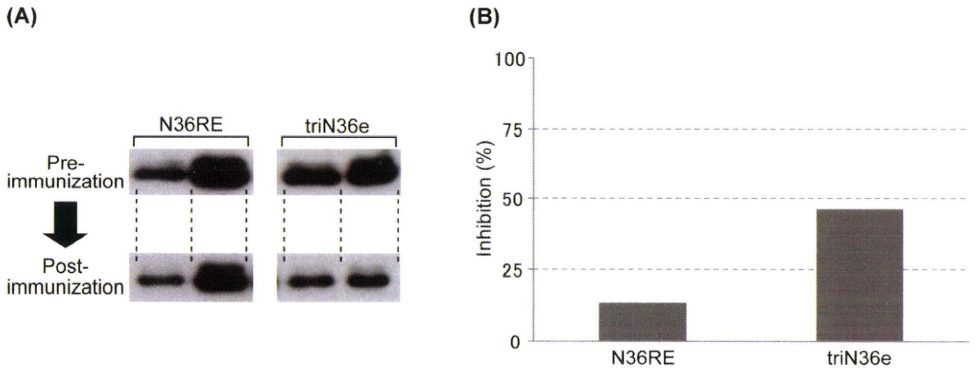

Figure 5. Determination of neutralization activity of the antibodies produced by immunization of peptidomimetic antigens. (A) Results of p24 assay to evaluate inhibition for HIV-1 infection by produced antibodies. Preimmunization sera were used as control. Experiments were duplicated. (B) Average % inhibition of p24 production calculated from the band intensities in panel (A).

of structure-specific antibody is still not clear, but the results could suggest the efficacy of producing antibodies with structural specificity and that the synthesis of structure-involving antigens is an effective strategy when higher specificity is required.

Neutralizing activity of sera against HIV-1 infection was assessed by p24 assays utilizing antisera from two mice that showed antibody production for each antigen (Figure 5). Sera

Table 1. Differences of α-Helicities between N36RE and triN36e Calculated from CD Spectra in Figure [3]

	$[\theta]_{222}$	$[\theta]_{222}/[\theta]_{208}$	α-helicity
N36RE	−30 957	0.87	73%
triN36e	−38 998	0.96	95%

Table 2. EC_{50} and CC_{50} Values Calculated from Inhibition Assays of Peptidomimetics

	AZT	triN36e	N36RE
EC_{50} (μM)[a]	0.047	0.49	1.4
CC_{50} (μM)[b]	>50	>1	>10

[a] EC_{50} values are based on the inhibition of HIV-induced cytopathogenicity in MT-4 cells. [b] CC_{50} values are based on the reduction of the viability of MT-4 cells. All data are the mean values for at least three experiments.

from mice immunized with the same antigen showed similar inhibitory activity against viral infection (12.5% and 14.8% for N36RE, 40.3% and 52.1% for triN36e). A trend was observed that the sera from triN36e immunization shows higher inhibition than those from N36RE immunization. This suggests that the synthetic antigen corresponding to the N36 trimeric form induces antibody with neutralization activity superior to that of the monomer peptide antigen and implies a restricted response of B-cells upon immunization to the trimeric form of N36RE. In order to assess the compatibility of induced antibodies in HIV-1 entry inhibition, the HIV-1 inhibitory activities of peptidomimetics (N36RE and triN36e) have been evaluated by viral infection and cytotoxicity assays. A C-terminal region peptide known as Enfuvirtide (T20, Roche/Trimeris) has been used clinically as a fusion inhibitor, and its success indicates that gp41-derived peptides might be potent inhibitors, useful against HIV-1 infection (*30*). In the development of anti-HIV peptides, several mimetics such as Enfuvirtide, CD4 binding site of gp120 (*31*), and protein-nucleic acid interactions (*32*), which disrupt protein−protein interactions, have been produced. As indicated in Table 2, N36 and triN36e showed modest inhibitory activity as reported in previous studies (*33*−*35*). The potency of triN36e was three times higher than that of N36RE indicating that the active structure of monomer N36RE is a trimeric form. Cytotoxicity of the antigens was not observed at concentrations of 1 μM of triN36e and 10 μM of N36RE.

CONCLUSIONS

In summary, a mimic of HIV-1 gp41-N36 designed as a new vaccine has been synthesized utilizing a novel template with three branched linkers of equal lengths. Thiazolidine-forming ligation attached the esteraldehyde of three-branched template with N-terminal cysteine of peptides in an aqueous medium. The resulting peptide antigen successfully induces antibodies with neutralization activity against HIV-1 infection. It is of special interest that the antibody produced acquires structural preference to antigen, which showed 30 times higher binding affinity for trimer than for monomer. This indicates the effectiveness of the design based on the structural dynamics of HIV-1 fusion mechanism of an antigen which could elicit neutralizing antibodies. In a design based on the N36 region of gp41, the exposed timing of epitopes is limited during HIV-1 entry (*36*), and carbohydrates, which could make accession of antibodies to epitopes difficult, are not associated with the amino acid residues of the native protein. These two advantages could further enhance the potential of a vaccine design based on the N36 region. During preparation of the manuscript, a new HIV vaccine strategy was reported by Burton's group (*37*). The report describes the importance of antibody recognition for the trimer form of surface protein. The trimer-specific antibodies indicate broad and potent neutralization. The gp41 trimer-form specific antibody produced in this study could also obtain the corresponding properties. The elucidation of antibody-producing mechanisms and epitope recognition mode of antibodies in antiserum during HIV-1 entry will be addressed in future studies.

ACKNOWLEDGMENT

The authors deeply thank Prof. K. Akiyoshi (Tokyo Medical and Dental Univ.) for allowing access to CD spectroporalimeter.

Supporting Information Available: HPLC chromatograms and NMR charts of compounds **3**, **5**, and **6**. Results of ESI-TOF-MS, and HPLC chromatograms of peptides N36RE, N36REGC, and triN36e. Results of serum titer ELISA of antisera collected during immunization. This material is available free of charge via the Internet at http://pubs.acs.org.

LITERATURE CITED

(1) Cabezas, E., Wang, M., Parren, P. W. H. I., Stanfield, R. L., and Satterthwait, A. C. (2000) A structure-based approach to a synthetic vaccine for HIV-1. *Biochemistry 39*, 14377–14391.

(2) Burton, D. R., Barbas, C. F., III, Persson, M. A. A., Koenig, S., Chanock, R. M., and Lerner, R. A. (1991) A large array of human monoclonal antibodies to type 1 human immunodeficiency virus from combinatorial libraries of asymptomatic seropositive individuals. *Proc. Natl. Acad. Sci. U.S.A. 88*, 10134–10137.

(3) Conley, A. J., Kessler, J. A. II, Boots, L. J., Tung, J. S., Arnold, B. A., Keller, P. M., Shaw, A. R., and Emini, R. A. (1994) Neutralization of divergent human immunodeficiency virus type 1 variants and primary isolates by IAM-41−2F5, an anti-gp41 human monoclonal antibody. *Proc. Natl. Acad. Sci. U.S.A. 91*, 3348–3352.

(4) Ofek, G., Tang, M., Sambor, A., Katinger, H., Mascola, J. R., Wyatt, R., and Kwong, P. D. (2004) Structure and mechanistic analysis of the anti-human immunodeficiency virus type 1 antibody 2F5 in complex with its gp41 epitope. *J. Virol. 78*, 10724–10737.

(5) Alam, S. M., McAdams, M., Boren, D., Rak, M., Scearce, R. M., Gao, F., Camacho, Z. T., Gewirth, D., Kelsoe, G., Chen, P., and Haynes, B. F. (2007) The role of antibody polyspecificity and lipid reactivity in binding of broadly neutralizing anti-HIV-1 envelope human monoclonal antibodies 2F5 and 4E10 to glycoprotein 41 membrane proximal envelope epitopes. *J. Immunol. 178*, 4424–4435.

(6) Nelson, J. D., Brunel, F. M., Jensen, R., Crooks, E. T., Cardoso, R. M. F., Wang, M., Hessell, A., Wilson, I. A., Binley, J. M., Dawson, P. E., Burton, D. R., and Zwick, M. B. (2007) An affinity-enhanced neutralizing antibody against the membrane-proximal external region of human immunodeficiency virus type 1 gp41 recognizes an epitope between those of 2F5 and 4E10. *J. Virol. 81*, 4033–4043.

(7) Cardoso, R. M. F., Zwick, M. B., Stanfield, R. L., Kunert, R., Binley, J. M., Katinger, H., Burton, D. R., and Wilson, I. A. (2005) Broadly neutralizing anti-HIV antibody 4E10 recognizes a helical conformation of a highly conserved fusion-associated motif in gp41. *Immunity 22*, 163–173.

(8) Trkola, A., Purtscher, M., Muster, T., Ballaun, C., Buchacher, A., Sullivan, N., Srinivasan, K., Sodroski, J., Moore, J. P., and Katinger, H. (1996) Human monoclonal antibody 2G12 defines a distinctive neutralization epitope on the gp120 glycoprotein of human immunodeficiency virus type 1. *J. Virol. 70*, 1100–1108.

(9) Pantophlet, R., Saphire, E. O., Poignard, P., Parren, P. W. H. I., Wilson, I. A., and Burton, D. R. (2003) Fine mapping of the interaction of neutralizing and nonneutralizing monoclonal antibodies with the CD4 binding site of human immunodeficiency virus type 1 gp120. *J. Virol. 77*, 642–658.

(10) Sanders, R. W., Vesanen, M., Schuelke, N., Master, A., Schiffner, L., Kalyanaraman, R., Paluch, M., Berkhout, B., Maddon, P. J., Olson, W. C., Lu, M., and Moore, J. P. (2002) Stabilization of the soluble, cleaved, trimeric form of the envelope glycoprotein complex of human immunodeficiency virus type 1. *J. Virol. 76*, 8875–8889.

(11) Yang, X., Wyatt, R., and Sodroski, J. (2001) Improved elicitation of neutralizing antibodies against primary human immunodeficiency viruses by soluble stabilized envelope glycoprotein trimers. *J. Virol. 75*, 1165–1171.

(12) Grundner, C., Mirzabekov, T., Sodroski, J., and Wyatt, R. (2002) Solid-phase proteoliposomes containing human immunodeficiency virus envelope glycoproteins. *J. Virol. 76*, 3511–3521.

(13) De Rosny, E., Vassell, R., Wingfield, R. T., Wild, C. T., and Weiss, C. D. (2001) Peptides corresponding to the heptad repeat motifs in the transmembrane protein (gp41) of human immunodeficiency virus type 1 elicit antibodies to receptor-activated conformations of the envelope glycoprotein. *J. Virol. 75*, 8859–8863.

(14) Tam, J. P., and Yu, Q. (2002) A facile ligation approach to prepare three-helix bundles of HIV fusion-state protein mimetics. *Org. Lett. 4*, 4167–4170.

(15) Xu, W., and Taylor, J. W. (2007) A template-assembled model of the N-peptide helix bundle from HIV-1 gp-41 with high affinity for C-peptide. *Chem. Biol. Drug Des. 70*, 319–328.

(16) Louis, J. M., Nesheiwat, I., Chang, L., Clore, G. M., and Bewlet, C. A. (2003) Covalent trimers of the internal N-terminal trimeric coiled-coil of gp41 and antibodies directed against them are potent inhibitors of HIV envelope-mediated cell fusion. *J. Biol. Chem. 278*, 20278–20285.

(17) Chen, Y.-H., Yang, J. T., and Chau, K. H. (1974) Determination of the helix and β form of proteins in aqueous solution by circular dichroism. *Biochemistry 13*, 3350–3359.

(18) Gans, P. J., Lyu, P. C., Manning, M. C., Woody, R. W., and Kallenbach, N. R. (1991) The helix-coil transition in heterogeneous peptides with specific side-chain interactions: theory and comparison with CD spectral data. *Biopolymers 13*, 1605–1614.

(19) Jackson, D. Y., King, D. S., Chmielewski, J., Singh, S., and Schultz, P. G. (1991) A general approach to the synthesis of short alpha-helical peptides. *J. Am. Chem. Soc. 113*, 9391–9392.

(20) Ohba, K., Ryo, A., Dewan, M. Z., Nishi, M., Naito, T., Qi, X., Inagaki, Y., Nagashima, Y., Tanaka, Y., Okamoto, T., Terashima, K., and Yamamoto, N. (2009) Follicular dendritic cells activate HIV-1 replication in monocytes/macrophages through a juxtacrine mechanism mediated by P-selectin glycoprotein ligand 1. *J. Immunol. 183*, 524–532.

(21) Liu, J., Shu, W., Fagan, M. B., Nunberg, J. H., and Lu, H. (2001) Structural and functional analysis of the HIV gp41 core containing an Ile573 to Thr substitution: implications for membrane fusion. *Biochemistry 40*, 2797–2807.

(22) Liu, C. F., and Tam, J. P. (1994) Peptide segment ligation strategy without use of protecting groups. *Proc. Natl. Acad. Sci. U.S.A. 91*, 6584–6588.

(23) Tam, J. P., and Miao, Z. (1999) Stereospecific pseudoproline ligation of N-terminal serine, threonine, or cysteine-containing unprotected peptides. *J. Am. Chem. Soc. 121*, 9013–9022.

(24) Tam, J. P., Yu, Q., and Yang, J.-L. (2001) Tandem ligation of unprotected peptides through thiaprolyl and cysteinyl bonds in water. *J. Am. Chem. Soc. 123*, 2487–94.

(25) Eom, K. D., Miao, Z., Yang, J.-L., and Tam, J. P. (2003) Tandem ligation of multipartite peptides with cell-permeable activity. *J. Am. Chem. Soc. 125*, 73–82.

(26) Sadler, K., Zhang, Y., Xu, J., Yu, Q., and Tam, J. P. (2008) Quaternary protein mimetics of gp41 elicit neutralizing antibodies against HIV fusion-active intermediate state. *Biopolym. (Pept. Sci.) 90*, 320–329.

(27) Bychkova, V. E., Dujsekina, A. E., Klenin, S. I., Tiktopulo, E. I., Uversky, V. N., and Ptitsyn, O. B. (1996) Molten globule-like state of cytochrome *c* under conditions simulating those near the membrane surface. *Biochemistry 35*, 6058–6063.

(28) Nishi, K., Komine, Y., Sakai, N., Maruyama, T., and Otagiri, M. (2005) Cooperative effect of hydrophobic and electrostatic forces on alcohol-induced α-helix formation of α_1-acid glycoprotein. *FEBS Lett. 579*, 3596–3600.

(29) Chan, D. C., Chutkowski, C. T., and Kim, P. S. (1998) Evidence that a prominent cavity in the coiled coil of HIV type 1 gp41 is an attractive drug target. *Proc. Natl. Acad. Sci. U.S.A. 95*, 15613–15617.

(30) Liu, S., Jing, W., Cheng, B., Lu, H., Sun, J., Yan, X., Niu, J., Farmar, J., Wu, S., and Jiang, S. (2007) HIV gp41 C-terminal heptad repeat contains multifunctional domains: relation to mechanism of action of anti-HIV peptides. *J. Biol. Chem. 282*, 9612–9620.

(31) Franke, R., Hirsch, T., Overwin, H., and Eichler, J. (2007) Synthetic mimetics of the CD4 binding site of HIV-1 gp120 for the design of immunogens. *Angew. Chem., Int. Ed. 46*, 1253–1255.

(32) Robinson, J. A. (2008) β-hairpin peptidomimetics: design, structures and biological activities. *Acc. Chem. Res. 41*, 1278–1288.

(33) Lu, M., Ji, H., and Shen, S. (1999) Subdomain folding and biological activity of the core structure from human immunodeficiency virus type 1 gp41: implications for viral membrane fusion. *J. Virol. 73*, 4433–4438.

(34) Eckert, D. M., and Kim, P. S. (2001) Design of potent inhibitors of HIV-1 entry from the gp41 N-peptide region. *Proc. Natl. Acad. Sci. U.S.A. 98*, 11187–11192.

(35) Bianchi, E., Finotto, M., Ingallinella, P., Hrin, R., Carella, A. V., Hous, X. S., Schleif, W. A., and Miller, M. D. (2005) Covalent stabilization of coiled coils of the HIV gp41 N region yields extreamely potent and broad inhibitors of viral infection. *Proc. Natl. Acad. Sci. U.S.A. 102*, 12903–12908.

(36) Zwick, M. B., Saphire, E. O., and Burton, D. R. (2004) gp41: HIV's shy protein. *Nat. Med. 10*, 133–134.

(37) Walker, L. M., Phogat, S. K., Chan-Hui, P.-Y., Wagner, D., Phung, P., Goss, J. L., Wrin, T., Simek, M. D., Fling, S., Mitcham, J. L., Lehrman, J. K., Priddy, F. H., Olsen, O. A., Frey, S. M., Hammond, P. W., Kaminsky, S., Zamb, T., Moyle, M., Koff, W. C., Poignard, P., and Burton, D. R. (2009) Broad and potent neutralizing antibodies from an African donor reveal a new HIV-1 vaccine target. *Science 326*, 285–289.

BC900502Z

本城 咲季子，西田 栄介
（京都大学大学院生命科学研究科シグナル伝達学分野）

The mechanisms underlying dietary restriction-induced longevity

Sakiko Honjoh and Eisuke Nishida (Department of Cell and Developmental Biology, Graduate School of Biostudies, Kyoto University, Kitashirakawaoiwake-cho, Sakyo-ku, Kyoto 606-8502, Japan)

エピジェネティクな遺伝子発現制御のためのDNAメチル化酵素の創製

1. はじめに

セントラルドグマの提唱以来，遺伝子情報と生体機能の制御にまつわる生体分子およびその修飾が注目されてきた．エピジェネティクス分野における研究では，翻訳後のタンパク質修飾(リン酸化，メチル化，アセチル化など)，RNAによる転写調節などと併せて遺伝子のメチル化が重要な研究対象である．哺乳類細胞ではシトシンの5′位がメチル化を受け，ヒト細胞内では実に7割のCpG配列がメチル化を受けていることが明らかにされている．遺伝子でのメチル化の役割は遺伝子情報の読み出しの制御が主なものである．メチル化を受けているCpG配列にはメチル化シトシン結合タンパク質が結合し，さらにタンパク質複合体が形成され，クロマチンの脱アセチル化が促進される．脱アセチル化を受けた部位ではクロマチン構造が密な状態となり遺伝子の転写がオフの状態になる．DNAメチル化はゲノムDNAの機能制御において重要な役割を果たしており，胚発生時に行われるゲノムインプリンティングは細胞の運命を司るコードとしてその解明が急速に進んでいる．がん細胞においてメチル化パターンの異常がみられることから，DNAメチル化は細胞のがん化に密接に関わるとされている．また，最近ではメチル化パターンと細胞のリプログラミングの関連が注目されている．このようにDNAメチル化はDNA機能の一端を担っていることから，人為的にメチル化を制御することの重要性が認識されている．本稿ではエピジェネティクス分野においてDNAメチル化に関連した最近の研究の動向，特に人工的なメチル化制御に関して解説する．

2. 研究の背景

メチル化されたシトシン塩基はメチル化シトシン結合タンパク質（MeCP2）によって認識され，MeCP2が他のタンパク質との会合体を形成し，ヒストンの脱アセチル化を行う．これによりヒストンの構造変化が誘起された部分のゲノム遺伝子では転写反応が抑制を受ける．シトシン塩基のメチル化は細胞分裂後も保存されるので，永久的にこの転写抑制が保存される．遺伝子の転写抑制はRNAiや転写抑制ドメインを用いる方法などで一時的な制御は可能であるが，細胞分裂後も保存される永久的な抑制を可能にするのがシトシンのメチル化であると考えられる[1]．シトシンのメチル化はがん細胞中の特定の配列で高頻度に観察される（図1A，B）[2]．このため，メチル化反応を人工的に制御することは有効な疾病治療の選択肢になると考えられている．このような遺伝子に対する人工的な制御を行うためには任意の標的とするDNA配列に結合するタンパク質が必要である．この役割に最適なタンパク質としてZnフィンガータンパク質に対する注目が高まっている．

Znフィンガータンパク質はその発見から四半世紀を経て，遺伝子を標的とした医療への応用が現実味を帯びてきている．Znフィンガードメインは約30アミノ酸で構成されββα構造のαヘリックス中のアミノ酸側鎖がDNAの3塩基を認識する．このモジュール構造がタンデムに連結されることから非対称かつ長鎖のDNA配列の認識が可能になる[3]．これまでにファージディスプレイ法や酵母ツーハイブリッド法などを用いて大規模なライブラリー中から各コドン配列に対応するドメインが選択され，それらを組み合わせることで標的とする遺伝子配列に対して特異的に結合するDNA結合ドメインを構築することが可能となっている[4]．こうした任意の標的DNA配列に結合するように“プログラム”できるという特徴を持つDNA結合ドメインはZnフィンガーのみであり，DNAを修飾する酵素に融合することで酵素の働きを制御することができるということが示されている．応用例としてDNAに働く酵素ドメインとの融合タンパク質がこれまでに数種類報告されている．DNA切断酵素，DNA組換え酵素，そしてDNAメチル化酵素がそれらの例であり，メチル化酵素については1997年に*Sss*Iとの融合体を用いたDNAメチル化に関する報告がなされた[5]．他の2種類の酵素との大きな違いとしてDNAメチル化酵素はDNA結合機能と酵素活性機能がリンクしているという点がある．すなわち，同じ構造中に二つの機能に関与するアミノ酸残基が含まれている．

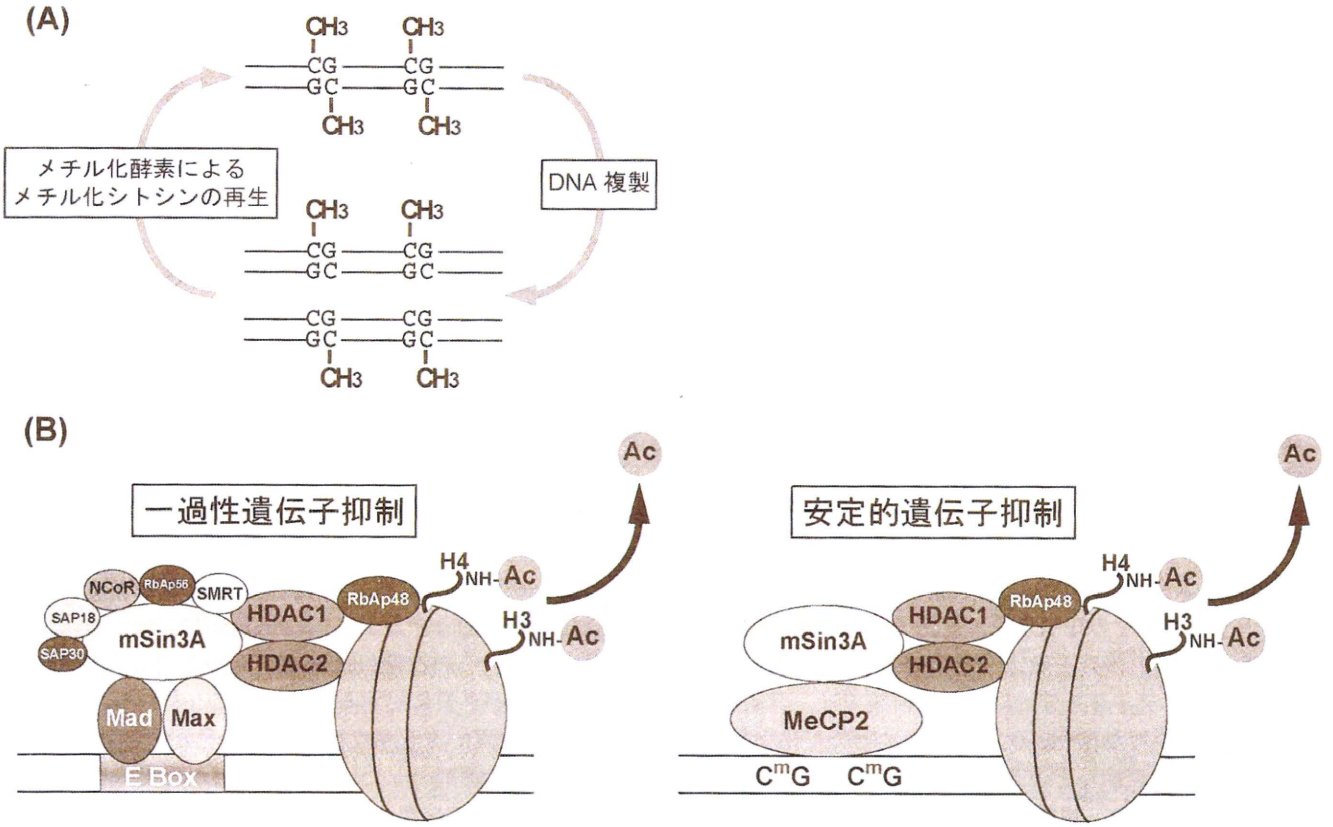

図1 (A)メチル化シトシンの保持機構について．(B)CpG メチル化による転写抑制機構と転写抑制因子群の働きの比較．一過性の抑制因子群は生理的条件の変化に応じて形成される（左）．一例として E Box などの抑制エレメント配列を Mad–Max ヘテロ二量体やホルモンレセプターが認識し，それらがコリプレッサー mSin3A と相互作用する．mSin3A は 8 種類のタンパク質と相互作用する．これらの中に含まれる SMRT は HDAC1 および HDAC2 や HDAC1 とヒストン H4 との間を架橋する RbAp48 と相互作用する．デアセチラーゼはヒストン H3，H4 上の脱アセチル基を促進する．メチル化の関与する安定的な遺伝子抑制では CpG メチル化に対して MeCP2 が結合することで開始される．MeCP2 は mSin3A と相互作用する．以下の機構は一過性のものと同様であると考えられているが明らかにされていない部分もある．

従って，全長のメチル化酵素と Zn フィンガータンパク質を融合したものではメチル化酵素の DNA 認識能に由来する高いバックグラウンド反応が見られるという克服すべき課題があった[5~8]．

3. タンパク質ドメイン分割法の DNA メチル化酵素への応用

近年になって，タンパク質ドメインを分割型にしてその機能を抑制し，タンパク質間もしくはタンパク質–核酸などの相互作用によって各分割ドメインが近傍に存在する場合に再会合が起こり，タンパク質ドメインの機能が回復する方法（protein-fragment complementation assays）がユビキチンについて最初に報告された[9]．この方法を酵素ドメインや蛍光タンパク質に適用することで細胞内シグナルの可視化などに有効な手段になると期待されている[10,11]．原核細胞由来の DNA メチル化酵素である *Hha*I methyltransferase（M.*Hha*I）は 327 アミノ酸で構成されるが，N 末端側ドメイン（1–240）と C 末端ドメイン（210–327）に分割することで自己会合型ドメインにできることが報告されている[12]．M.*Hha*I の認識 DNA 配列は GCGC であり，CpG 配列のシトシン塩基をメチル化する．4 塩基という短い認識配列のため，ゲノム DNA に対しては無数にその標的配列が存在する．著者らは DNA 認識特異性を向上させることで，ゲノム DNA 中においても 1 箇所の特定部位のみをメチル化する酵素を構築できるのではないかと考えた．そこで，Zn フィンガードメインを利用して DNA 結合機能に高い配列選択性を付与して DNA 配列に応じた酵素ドメインの再会合を可能にすることで，ゲノム DNA 中の特定部位でメチル化反応を行う人工酵素の開発を試みた（図 2A）．

4. 分割型DNAメチル化酵素の機能

分割型メチル化酵素機能の解析のためにアラビノース制御プロモーター下流の2箇所にShine-Dalgarno配列を配置したプラスミドベクターを作製し，同時に発現が行えるシステムを構築した．分割ドメインに9塩基を認識するZnフィンガードメインを7アミノ酸からなるリンカー配列を介して融合した．コントロールとしてN末端ドメインのみ，ZnフィンガードメインとM.*Hha*I酵素全長の融合体，M.*Hha*Iを用意した(図2B)．ウェスタンブロットの結果，大腸菌内での発現は分割型酵素の両ドメインにおいて十分な量が得られていることが明らかになった．メチル化反応の解析には*Hha*I制限酵素(R.*Hha*I)による切断を用いた．R.*Hha*IはM.*Hha*Iと同じDNA配列（GCGC）を認識し，配列中のCpGでのメチル化に感受性を持つため，シトシン塩基がメチル化されている場合は切断が阻害される．タンパク質発現ベクターにZnフィンガードメインの標的配列を含むGCGC配列を組み込み，このサイトでのみメチル化が行われている場合にプラスミドのR.*Hha*I処理によって1467塩基対のフラグメントが生成されるシステムとした（図2C)．この発現ベクターには他に18箇所のGCGC配列が含まれるので，メチル化のバックグラウンド反応なども容易に検出できる．分割型メチル化酵素の反応ではR.*Hha*Iによる切断の阻害を示す1467bpのバンドが現われた．分割ドメインの会合によってメチル化が行われていることを確認するためにN末端ドメインのみを用いたところ，R.*Hha*Iでの切断の阻害は観察されず，GCGC標的配列でのメチル化には2ドメインの会合が必要であることが示された．コントロールのM.*Hha*IドメインとZnフィンガードメインの融合体では，プラスミド上の全てのGCGCサイトでのR.*Hha*Iによる切断の阻害が確認された．この結果は，これまでの酵素ドメイン全長とZnフィンガーモチーフの融合体に関する研究で報告されている通り，M.*Hha*I自体のDNA結合親和性の影響が大きく，DNA配列に対して非特異的なメチル化が行われていることを示すもので，我々の新たに開発した分割型メチル化酵素のDNA配列に対する特異性の高さが示された(図2C)．また，M.*Hha*Iドメインのみの発現においても全長型酵素(B-4）と同様の結果が得られた．

バイサルファイト反応はシトシン塩基をウラシル塩基に置換する反応であり，メチル化されたシトシンは反応を受けない．バイサルファイト反応後のDNAにPCRを行うと，シークエンス解析の際に修飾を受けていないシトシンはチミンとして，メチル化を受けているシトシンはそのまま検出される．この手法を用いて，分割型メチル化酵素のDNA配列特異的なメチル化反応を検出した．その結果，N末端ドメインのみではメチル化は観察されないが，全長融合型および分割型メチル化酵素の場合では標的配列でのシトシンメチル化が観察された．さらに標的配列以外のGCGC配列では全長融合型のみでメチル化が観察され，分割型メチル化酵素の標的配列に対する特異性の高さが確認された[13]（図2D)．

5. その他の標的配列特異的メチル化酵素

ドメイン分割法を用いる以外にもDNAメチル化酵素の配列特異性を向上させる試みが行われている．その例として全長型のメチル化酵素の配列特異性を向上させる方法としてバックグラウンド反応を抑制する方法がある．これはすなわち，アミノ酸変異を導入してメチル化酵素活性を抑えることでZnフィンガーによるDNA認識を優位に働かせることが可能になる方法である．このメチル化酵素を哺乳類細胞内において発現させ，標的配列におけるメチル化反応とヒストンメチル化の変化量を定量した結果，標的配列周辺におけるメチル化は上昇し，ヒストンメチル化に関してもH3K4Me3の減少とH3K9Me2の増加が確認された．また，このようなZnフィンガー融合型メチル化酵素を用いて哺乳類細胞内での転写抑制が行われることも示されている．

6. 今後の展望

我々が開発した分割型メチル化酵素はこれまでの全酵素ドメインとの融合体に比べて，標的配列に対する特異性という点において優れた結果を示すことができた（図3)．DNA配列に対するZnフィンガーモチーフによる特異的な結合を用いた分割型酵素の再会合はGFP，β-lactamaseを用いて行われた例がある[14]．これらは，ドメイン間の再会合がゲノムDNA上において可能である場合，一塩基多型などのレポーターとして非常に有望である．しかし，いずれの例においても*in vitro*での機能を示すだけにとどまっていた．今回我々が行った*in vivo*での分割型酵素の再会合は最初の例であり，今後の哺乳類細胞内での応用に期待を抱いている．また，DNA配列に対する修飾反応であるという点においても最初の例であり，ナノテクノロジー分野における応用も可能であると考えられる．DNAメチル化酵素は補因子となる*S*-アデノシル-L-メチオニンの誘導体を取り込んで，酵素反応を行うことで特定の

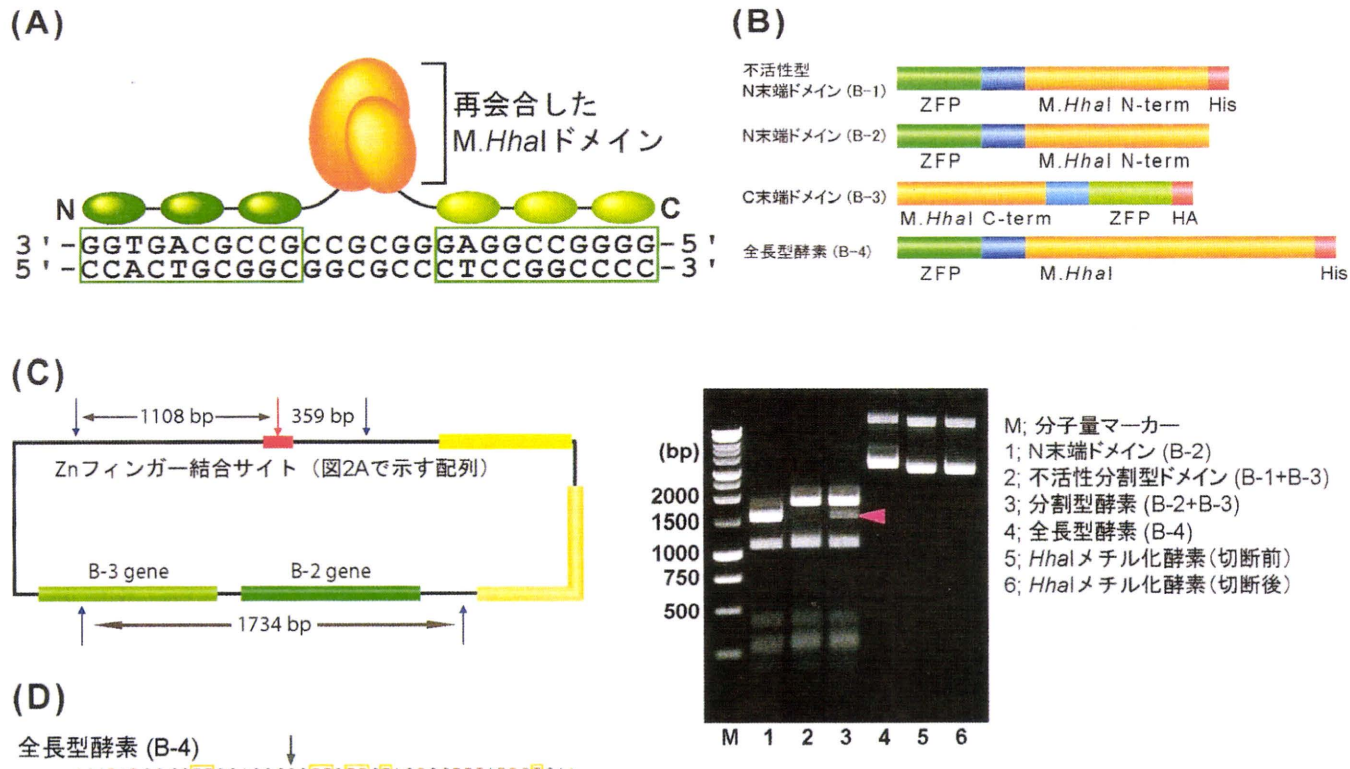

図2 (A)構築した分割型メチル化酵素のモデル図．標的DNA配列に対してZnフィンガーが結合し，その間のGCGC配列がメチル化を受ける．(B)実験に用いた分割型酵素及び融合体の概要．分割型酵素にはB-1もしくはB-2とB-3の組み合わせを用いた．それぞれZFP；Znフィンガードメイン，M.*Hha*I N-term；*Hha*Iメチル化酵素のN末端側ドメイン（1–240），M.*Hha*I C-term；*Hha*Iメチル化酵素のC末端側ドメイン（210–327），His；ヒスチジンタグ，HA；HAタグを表す．青色はリンカー配列部分を表す．不活性型N末端ドメインはC末端にヒスチジンタグが付加しているため再会合を阻害すると考えられた．(C)*Hha*I制限酵素切断によるメチル化反応検出に用いたプラスミド（左）とその検出結果（右）．青矢印で示したのは主な*Hha*I切断部位であり，赤矢印はZnフィンガー標的サイト中の*Hha*I切断部位を示す．配列特異的なメチル化が起きている場合は赤矢印部分は切断を受けず，レーン3で示すようなフラグメントが検出された．また，他の*Hha*I切断部位も非特異にメチル化を受けている場合はプラスミドが切断されず，レーン4またはレーン6のような結果となった．(D)バイサルファイトシークエンス解析によるGCGC標的配列でのメチル化反応解析．

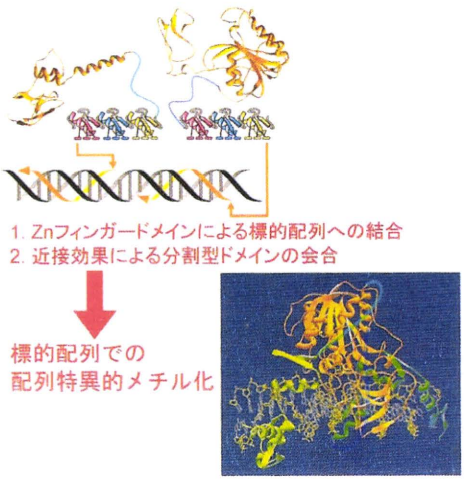

図3 分割型メチル化酵素によるDNA配列特異的なメチル化反応の概要と標的DNA配列上での再会合の予測図[12]

DNA配列に対するタグ付けが可能である[15]．従って，分割型メチル化酵素の基質結合ポケットの最適化によって，配列特異的なDNA標識が行えると考えられる．分割型メチル化酵素の機能解析については現在，*in vitro* での解析および哺乳類細胞内における機能という両面からのアプローチを展開している．

Znフィンガータンパク質のDNA配列に対する特異性を利用した標的遺伝子マニピュレーションではDNA切断酵素が医療への実用化という面において一歩リードしている．今後は，他の酵素（組換え酵素，メチル化酵素など）もそれぞれの特長を生かして，医療分野でのニーズに即した実用性のある研究展開が行われることが期待される．

1) Bird, A. (2002) *Genes Dev.*, **16**, 6–21.
2) Esteller, M. (2007) *Nat. Rev. Genet.*, **8**, 286–298.
3) Hirata, T., Nomura, W., Imanishi, M., & Sugiura, Y. (2005) *Bioorg. Med. Chem. Lett.*, **15**, 2197–2201.
4) Segal, D.J., Beerli, R.R., Blancafort, P., Dreier, B., Effertz, K., Huber, A., Koksch, B., Lund, C.V., Magnenat, L., Valente, D., & Barbas, C.F., III (2003) *Biochemistry*, **42**, 2137–2148.
5) Xu, G.L. & Bestor, T.H. (1997) *Nat. Genetics*, **17**, 376–378.
6) Carvin, C.D., Parr, R.D., & Kladde, M.P. (2003) *Nucleic Acids Res.*, **31**, 6493–6501.
7) Li, F., Papworth, M., Minczuk, M., Rohde, C., Zhang, Y., Ragozin, S., & Jeltsch, A. (2007) *Nucleic Acids Res.*, **35**, 100–112.
8) Smith, A.E., Hurd, P.J., Bannister, A.J., Kouzarides, T., & Ford, K.G. (2008) *J. Biol. Chem.*, **283**, 9878–9885.
9) Johnsson, N. & Varshavsky, A. (1994) *Proc. Natl. Acad. Sci. U.S.A.*, **91**, 10340–10344.
10) Magliery, T.J., Wilson, C.G., Pan, W., Mishler, D., Ghosh, I., Hamilton, A.D., & Regan, L. (2005) *J. Am. Chem. Soc.*, **127**, 146–157.
11) Galarneau, A., Primeau, M., Trudeau, L.E., & Michnick, S.W. (2002) *Nat. Biotechnol.*, **20**, 619–622.
12) Choe, W., Chandrasegaran, S., & Ostermeier, M. (2005) *Biochem. Biophys. Res. Commun.*, **334**, 1233–1240.
13) Nomura, W. & Barbas, C.F., III (2007) *J. Am. Chem. Soc.*, **129**, 8676–8677.
14) Ghosh, I., Stains, C.I., Ooi, A.T., & Segal, D.J. (2006) *Mol. Biosyst.*, **2**, 551–560.
15) Lukinavicius, G., Lapine, V., Stasevskij, Z., Dalhoff, C., Weinhold, E., & Klimasauskas, S. (2007) *J. Am. Chem. Soc.*, **129**, 2758–2759.

野村 渉[1]，増田 朱美[1,2]，玉村 啓和[1,2]
（[1]東京医科歯科大学生体材料工学研究所，
[2]東京医科歯科大学大学院疾患生命科学研究部）

Development of site-specific DNA methylase for epigenetic regulation of gene expression

Wataru Nomura[1], Akemi Masuda[1,2] and Hirokazu Tamamura[1,2] ([1]Institute of Biomaterials and Bioengineering, Tokyo Medical and Dental University, [2]Graduate School of Biomedical Science, Tokyo Medical and Dental University, 2–3–10 Kandasurugadai, Chiyoda-ku, Tokyo 101–0062, Japan)

植物における小分子RNAの動態制御

1. 植物における小分子RNAの発見

線虫においてlin-4，let-7といった小分子RNAが発見されると，これがきっかけとなりショウジョウバエからヒト，さらにはシロイヌナズナ，イネなどの植物にも21塩基長ほどの小分子RNAが多く発見されるようになった．

そのなかでmicroRNA（miRNA）は19–24塩基長の非翻訳RNAとして動物，植物で広く知られるようになった．miRNAは相補的な配列をもった標的mRNAと結合し，そのmRNAの分解あるいは翻訳抑制を導き[1]，遺伝子の発現のon/offを微調整する．miRNA/標的mRNA制御系は多くの遺伝子に関係することが明らかとなるにつれ，今では真核生物の遺伝子発現において広く一般的に用いられているもので，制御の緻密さを与えているものとして考えられるようになった[2]．遺伝子の数が問題なのではなく，いかにしてそれらを使うか，抑えるかが，生物が進化するうえで重要だったのであろう．

植物の形態形成について，最近分子レベルでの研究が進展し理解が進んでいる．そしてオーキシンなどの植物ホルモンの作用，組織間の信号伝達が関与する形態形成や環境応答における遺伝子発現制御にもmiRNAが関与していることが明らかとなっている[3]．たとえば植物の茎の先端には茎頂分裂組織があって，そこには分裂を続ける主な細胞が存在する．そこから，分裂を続ける細胞群と，未分化状態からはずれて組織の分化へと向かう細胞群とが生まれていく．上下，向背性・向腹性（葉の表裏など）などの軸方向に沿って運命の異なる複数の組織，細胞群が生み出さ

2O-11

Effects of DNA binding and linker length on recombination of artificial zinc-finger recombinase

Akemi Masuda[1, 2], Wataru Nomura[1]*, Arisa Urabe[1] and Hirokazu Tamamura[1, 2]*

[1]Institute of Biomaterials and Bioengineering, Tokyo Medical and Dental University, [2]Graduate School of Biomedical Science, Tokyo Medical and Dental University

ABSTRACT

Utilizing sequence-specificity of DNA recognition of zinc finger proteins (ZFPs), zinc finger recombinases (RecZF) can be constructed. Recombinases would be powerful tools of gene knockout. For the design of highly-active RecZF, effects of binding affinity of ZFPs and linker length connecting ZFP and a catalytic domain on recombination were studied. The obtained results show that these factors are important for recombination in addition to activity of catalytic domains.

INTRODUCTION

Artificial ZFPs consist of Cys_2-His_2-type modules connected by short linkers. The module is composed of approximetely 30 amino acids and forms a ββα structure by coordination of zinc ion. Several zinc-finger chimera enzymes including nucleases (1), recombinases (2, 3), and methylases (4) have been constructed. Utilization of ZFP as a DNA binding domain of artificial enzymes is a powerful strategy for DNA manipulation. Therefore, applications of these enzymes in gene therapy are expected. For recombinases, an advantageous point over nucleases is that the sequences modified by recombination are predictable. Moreover, as the reaction is occurred by formation of tetramer during strand transfer, possibility of cytotoxicity often caused by off-target effects could be reduced (Fig. 1).

Tn3 resolvase belongs to a recombinase family. It has been shown that it is possible to construct aritificial recombinases by replacing the DNA binding domain with ZFP because the catalytic domain and the DNA binding domain of the resolvase are structurally separated (2). Additionally, a molecular evolution strategy has been employed to construct more active RecZFs (2). In this study, effects of module numbers of ZFPs and linker length between the catalytic domain and ZFP on recombination were evaluated utilizing both *E. coli* and mammalian cells. Since these factors would be omitted in molecular evolution study, it was expected that the reports would be useful for the design of efficient RecZF.

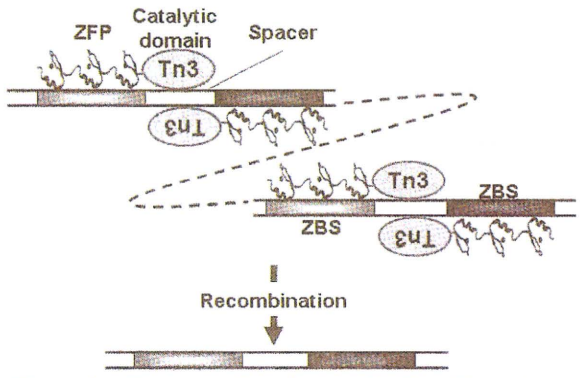

Fig. 1. Recombination of RecZF that excises a region between the target sites.

RESULTS AND DISCUSSION

Design of target sequences and evaluation of DNA binding affinity of ZFPs.

The target sites are composed of 20 bp spacer sequence flanked by 18 bp zinc-finger binding sites (ZBS) (Fig. 1). The spacer sequence has been reported as Z+4 site for NM-resolvase (2).

Plasmids encoding 2- to 6-fingers modules were constructed and these ZFPs were expressed in *E. coli*. The purified ZFPs were employed for ELISA to evaluate DNA binding affinity. The results showed that binding affinity increases approximately from 160 to 13 (nM for K_d) depending on numbers of finger modules.

Table 1. Recombination efficiency of finger-number variants in *E. coli* and in CHO-K1 cells.

Numbers of finger modules	Recombination in *E. coli* (%)	Recombination in mammalian cells (%)
2 fingers	0	6.2 ± 0.2
3 fingers	34 ± 1.2	11.8 ± 1.2
4 fingers	54 ± 0.6	16.1 ± 0.4
5 fingers	55 ± 0.8	19.3 ± 0.6
6 fingers	51 ± 3.1	14.9 ± 0.6
non-binding 5 fingers	n.d.[a]	5.2 ± 1.3

[a]not determined.

Efficiency of recombination in *E. coli*.

Recombination of RecZF in *E. coli* was tested utilizing a plasmid recombination system. Each plasmid consists of coding sequence for a RecZF variant and target sequences. In this system, RecZF expressed from plasmids recognize target sequences and perform recombination. After excision of the region between target sites by recombination, a shorter plasmid is produced. The efficiency of recombination was evaluated by restriction enzyme assays. The results indicated that increase of recombination efficiency depend on the numbers of finger modules (Table 1). Recombination efficiency of ZFPs corresponds to DNA binding affinity. Studies of variants of linker length showed that a 12-amino-acids linker has the highest recombination efficiency among 0-30 amino-acids linkers.

Recombination of RecZF in mammalian cells.

For evaluation of recombination efficiency in mammalian cells, a stable cell line of CHO-K1 expressing EGFP driven by a CMV promoter. The reporter cassette sequences are flanked by target sites. Utilizing this cell line, recombination efficiency is evaluated by a decrease of EGFP fluorescence. Transfection efficiency was evaluated by DsRed fluorescence. Because DsRed is encoded downstream of IRES after EGFP gene, the expression of EGFP can be normalized by DsRed fluorescence. Thus, the recombination is evaluated in a semi-quantitative manner. After 48 hours of transfection, intensity of fluorescence in the cells was detected by FACS analysis. As a result, cells containing recombinant gene were obtained. It was suggested that values of recombination efficiency obtained from *E. coli* and mammalian cells by RecZF were different; however, the tendency was similar in both systems (Table 1).

CONCLUSION

In this study, it was revealed that recombination efficiency can be improved by the design of RecZF involving numbers of zinc finger modules and length of the linker connecting ZFP and the catalytic domain. The improved RecZF will be applied for specific gene knockout in the future study.

REFERENCES

1. Miller, J. C. *et. al. Nat. Biotechnol.* **2007**, *25*, 778-785.
2. Akopikan, A.; He, J.; Boocock, M.R.; Stark, W. M. *Proc. Natl. Acad. Sci. U.S.A.* **2003**, *100*, 8688-8691.
3. Gordley, R. M.; Smith, J. D.; Gräslund, T.; Barbas, C. F., III *J. Mol. Biol.* **2007**, *367*, 802-813.
4. Nomura, W.; Barbas, C. F., III *J. Am. Chem. Soc.* **2007**, *129*, 8676-8677.

*Corresponding authors: (e-mail address) nomura.mr@tmd.ac.jp; tamamura.mr@tmd.ac.jp

L-63

Novel tag-probe pairs for fluorescent imaging of proteins in living cells

Wataru Nomura, Nami Ohashi, Atsumi Mori, Tetsuo Narumi, Tomohiro Tanaka, Akemi Masuda, Hiroshi Tsutsumi, Hirokazu Tamamura

Department of Medicinal Chemistry, Institute of Biomaterials and Bioengineering, Tokyo Medical and Dental University, Tokyo, Japan

Practical techniques of protein imaging via functional peptide tags are useful in the field of proteome and chemical biology. New tag-probe pairs based on leucine zipper peptides for labeling target proteins have been developed by us. These consist of an alpha-helical probe peptide with an environmental-sensitive fluorescent dye and two antiparallel alpha-helical tag peptides. Since hydrophobic cores of leucine zipper peptides can be adjusted to form hydrophobic pockets, fluorescent dyes might bind selectively to these pockets. Binding of the probe peptide to the tag peptides results in movement of the fluorophore from a hydrophilic to a hydrophobic environment inside the leucine zipper structure, causing a dramatic fluorescent change, mediated by the binding of the two peptides. The tag-probe pairs based on the leucine zipper peptides were designated as ZIP tag-probe pairs, and applied them to the fluorescent imaging of a cell surface protein CXCR4. Furthermore, development of crosslink-type ZIP tag-probe pairs, introduction of different dyes and their application to imaging of PKC in living cells have been performed.

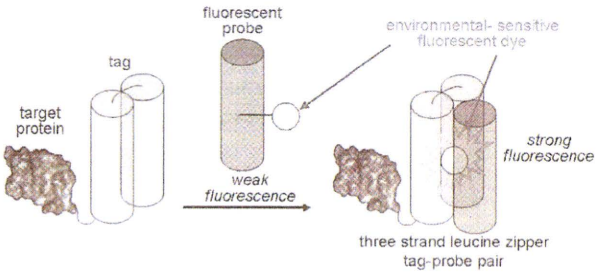

Tsutsumi H, Tamamura H, et al. *Angew. Chem., Int. Ed.* 2009, *48*, 9164.
Nomura W, Tamamura H, et al. *Biopolymers*. 2010, in press

P1-078

Synthesis and evaluation of CXCR4-derived peptides targeting the development of AIDS vaccines

Chie Hashimoto[1], Tetsuo Narumi[1], Wataru Nomura[1], Naoki Yamamoto[2], Hirokazu Tamamura[1]

1) Institute of Biomaterials and Bioengineering, Tokyo Medical and Dental University,
2) Yong Loo Lin School of Medicine, National University of Singapore

Despite enormous efforts in clinical researches, development of AIDS vaccine is greatly hampered by viral mutation. To overcome this problem, an immunotherapeutic approach targeting the HIV-1 co-receptor CCR5/CXCR4 has been proposed as an alternative immunization strategy for preventing HIV-1 infection. A chemokine receptor CXCR4, which belongs to GPCR, possesses an extracellular N-terminal region (Nt) and three extracellular loops (Ecls) on host cell surface, and the multiple interaction of Nt, Ecl-1 and 2 with a viral envelope glycoprotein gp120 is critical for the entry of HIV-1.
In this study, several peptide antigen molecules conjugated with a multiple-antigen peptide (MAP) derived from N-terminal region (Nt-1, 2 and 3) and extracellular loops (Ecl-1 and 2) were prepared, and their antibody titers were determined by ELISA for evaluation of their ability to induce CXCR4-specific antibodies. The Nt-1-derived peptide locating in the N-terminus of Nt and the Nt-3-derived peptide conjugated with MAP (Nt-3-MAP) exhibited significant antigenicity. The present results, including detail data which will be discussed in the symposium, are useful for the vaccine development.

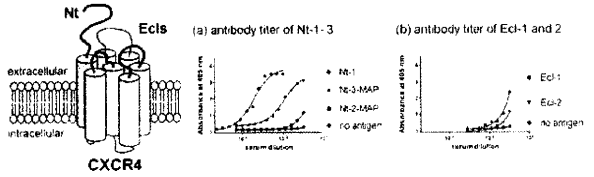

binding sites of ligands in CXCR4 dimers. Here, we present experimental results concerning the native state of CXCR4 dimer utilizing our bivalent ligands, leading to a clear comprehension of the precise structure. This approach could be utilized to any GPCRs as a molecular measure in design of bivalent ligands. Furthermore, fluorescent labeled bivalent ligands were applied to imaging of cancer cells expressing CXCR4.

P2-256

Development of a bivalent ligand for a chemokine receptor CXCR4 by utilizing polyproline helix as a linker

Wataru Nomura[1], Tomohiro Tanaka[1], Akemi Masuda[2], Tetsuo Narumi[1], Hirokazu Tamamura[1,2]

1) Institute of Biomaterials and Bioengineering, Tokyo Medical and Dental University, Tokyo, Japan,
2) Graduate School of Biomedical Science, Tokyo Medical and Dental University, Tokyo, Japan

A chemokine receptor CXCR4 belongs to the G-protein coupled receptor (GPCR) family. CXCR4 via interaction with its endogenous ligand, stromal-cell derived factor 1 (SDF-1)/CXCL12, induces various physiological functions in an embryonic stage: chemotaxis, angiogenesis, neurogenesis, etc. Recent studies have indicated a pivotal role of homo- and hetero-oligomerization of CXCR4 in cancer metastasis. Estimation of the precise distance between receptors in a dimer form will enable the efficient development of bivalent ligands of GPCRs, which have advantages in binding affinity and specificity. However, challenges in design of bivalent ligands have showed its difficulty because of the unclearness in dimeric forms of GPCRs. Therefore, there is an increasing demand for a novel strategy for this analysis. In this study, we designed and synthesized novel CXCR4 bivalent ligands with two FC131 analogues [cyclo(-D-Tyr-Arg-Arg-Nal-D-Cys-)] (Nal = L-3 (2-naphthyl)alanine) connected by a polyproline or a PEGylated polyproline linker. The linkers were expected to sustain a certain constant distance (2 - 8 nm) between the ligands. Our bivalent ligands with various linkers were applied to measure the distance between two